PHYLOGENOMICS OF ʻĒKAHA KŪ MOANA:

INSIGHTS FOR FUTURE BIODIVERSITY ASSESSMENTS

A THESIS SUBMITTED TO THE GRADUATE DIVISION OF THE UNIVERSITY OF HAWAIʻI AT MĀNOA IN PARTIAL FULFILLMENT OF THE REQUIREMENTS FOR THE DEGREE OF

MASTERS OF SCIENCE

IN

ZOOLOGY

DECEMBER 2023

By

Leah Elizabeth Kamilipua Shizuru

Thesis Committee:

Robert Toonen, Chairperson
Brian Bowen
Anthony Montgomery

To Gramma Kamilipua
(Lavaina Barbara Arthur Ferreira)

A hui hou.
I love you.

ACKNOWLEDGEMENTS

First and foremost, I want to express my heartfelt gratitude to my advisor, Rob Toonen, whose unwavering guidance, support, dedication, and knowledge have been indispensable throughout this academic journey. Your mentorship and encouragement haven't just shaped this research; they've been instrumental in my growth as a researcher. Thank you for believing in me.

I am very grateful to my committee members, Brian Bowen and Anthony (Tony) Montgomery, for their technical and field expertise, thought-provoking questions, intellectually stimulating discussions, and guidance in crafting this thesis.

I owe much to my earliest mentors at Kapiʻolani Community College: John Berestecky, Brian Hew, Robin Kaai, and Matthew Tuthill. They inspired my shift to natural sciences and provided crucial laboratory training and constant encouragement during my formative years. Other influential mentors during my undergraduate studies, Rosie Alegado, Kiana Frank, Shimi Claborn, and Keliʻi Kotubetey, introduced me to our culture and its depth, shaping my path further.

The success of this project hinged on the laboratory expertise of Clay Clark and the technicians at the IIGB Genomics Core facility at UC Riverside, who sequenced our initial libraries. Coral Lockerman & Mindy Mizobe at the Hawaiʻi Institute of Marine Biology (HIMB) prepared the libraries used in the final round of sequencing, while Jennifer Saito at the Advanced Studies in Genomics, Proteomics, and Bioinformatics at the University of Hawaiʻi sequenced our last group of libraries.

My heartfelt appreciation goes to the Council for Native Hawaiian Advancement, the Hayashida ʻohana, and the Schmidt Scholarship for their generous funding and unwavering support. Your financial assistance made this research possible and allowed me to contribute significantly to the field and community. The Schmidt Scholarship, particularly during my final year of graduate school, provided stability during a challenging period of family medical issues.

It's been an immense honor to be a part of the ToBo Lab and the wider community at Moku o Loʻe. I'm grateful for the incredible lab mates who were part of ToBo during my time at HIMB. Special thanks to the postdocs who mentored me: Ingrid Knapp, Claire Lewis, Jan Vicente, and Van Wishingrad.

To my ‘ohana: your love, encouragement, and support have been my anchor. Nainoa, your encouragement means the world to me. I am immensely proud of you, and I love you very much. Gramma Kamilipua, this work is dedicated to you; I wish you were here to witness its completion. Your unwavering support was invaluable. Mom and Dad, we made it!

Thank you to my friends who stood by me, offering encouragement, prayers, and unwavering support. Your friendship made the challenging journey through graduate school not just bearable but enjoyable.

Contributing to lāhui throughout this research has been an honor. This work signifies our collective commitment to preserving and advancing our cultural heritage, knowledge, and well-being. I hope the insights from this research may take us a step forward in addressing crucial conservation issues.

Finally, but by no means least, mahalo ke Akua. God, Your love knows no bounds.

ABSTRACT

Phylogenomics revolutionizes our understanding of evolutionary relationships among organisms by harnessing extensive genomic data. This approach provides unparalleled insights into evolutionary history by leveraging large-scale genomic data from multiple genes or entire genomes, arguably surpassing the limitations of single-gene studies. Phylogenomics offers enhanced accuracy and resolution, accounting for diverse genetic changes like mutations, insertions, deletions, and structural variations across genomes, ensuring robust evolutionary reconstructions. This method enables the elucidation of complex evolutionary patterns, estimation of species divergence times, and illumination of evolutionary processes such as adaptation and selection pressures. Moreover, phylogenomic studies are pivotal in informing conservation policies by delineating genetic relationships and evolutionary histories guiding efforts to understand biodiversity, genetic diversity, and adaptive potential. This thesis employed phylogenomic methods to assess the evolutionary relationships among antipatharians (black corals), specifically black corals (in Hawaiian ʻēkaha kū moana) collected across the Hawaiian Archipelago. The first thesis chapter details the discovery of the first mitogenome from *Cirrhipathes* (*Cirrhipathes* cf. *anguina* LS-2022), collected in Kauaʻi, Hawaiʻi, while the second chapter presents complete mitochondrial genomes from ten individuals across six antipatharian species (*Antipathes grandis*, *Antipathes griggi*, *Aphanipathes verticillata*, *Cirrhipathes* cf. *anguina*, *Myriopathes* cf. *ulex* and *Stichopathes* sp.) sampled from the Main and Northwestern Hawaiian Islands. These investigations provide critical insights into the evolutionary framework of ʻēkaha kū moana in the Hawaiian Archipelago, contributing substantially to our understanding of their genetic diversity.

TABLE OF CONTENTS

LIST OF FIGURES

CHAPTER 1

THE COMPLETE MITOCHONDRIAL GENOME OF A SPECIES OF BLACK CORAL GENUS *CIRRHIPATHES* DE BLAINVILLE, 1830 FROM KAUA‘I, HAWAI‘I (HEXACORALLIA: ANTIPATHARIA)

ABSTRACT

This chapter reports the first mitogenome from the antipatharian (black coral) genus *Cirrhipathes* (GenBank accession number ON653414). The 20,452 bp mitochondrial genome of *Cirrhipathes* cf. *anguina* LS-2022 consists of 13 protein-coding genes, two rRNA genes, and two tRNA genes (*trnM* and *trnW*). The mitogenome is typical of other antipatharian families, including an A+T biased (64.1%) base composition and cytochrome c oxidase subunit I (*COX1*) intron with embedded homing endonuclease gene (*HEG*). A phylogenetic tree based on complete mitogenome sequences of currently available antipatharians indicates *Cirrhipathes* cf. *anguina* LS-2022 is sister and closely related to *Stichopathes* sp. SCBUCN-8849 (Barrett et al. 2020). However, it seems unlikely that intergeneric taxa share 99.97% similarity across their complete mitogenomes, raising questions about the current taxonomy of this group. This chapter highlights the need for additional vouchered antipatharian species to be sequenced so phylogenetic relationships can be compared with accepted taxonomy.

INTRODUCTION

Antipatharians, commonly known as black corals, are globally distributed, slow-growing hexacorals (Cnidaria, Anthozoa) that occupy a broad bathymetric range (Wagner et al., 2012; Barrett et al., 2020). This morphologically variable order consists of 7 families, 49 genera, and 301 species (Molodtsova and Opresko, 2023). Though black corals are found as shallow as 2 m to over 8600 m, more than 75% of species occur below 50 m (Barrett et al., 2020). This predominance presents a logistic challenge to studying this order because most species are located at depths below the limit of conventional Self-Contained Underwater Breathing Apparatus (SCUBA) diving (Wagner, 2015). Limited ability to observe living specimens and access to samples leaves these organisms' basic biology and ecology largely unknown. Although they are less common on shallow-water reefs, in deeper waters these antipatharians are essential ecosystem engineers who create habitat for many species of vertebrates and invertebrates

(Wagner et al., 2012). In Hawai‘i, black corals are ecologically, culturally, and commercially important, and there has been an active commercial fishery for these corals since 1958 (Grigg, 2001) for use in the manufacture of precious coral jewelry. Black corals are the official gemstone of Hawai‘i and support a $30 million statewide precious coral industry (Grigg, 2004), which makes them the focus of considerable management interest for continued sustainable harvest. This mitogenome is the first for this genus and any Hawaiian antipatharian, thus establishing an essential foundation for future studies.

METHODS

The antipatharian sample used in this study (Fig 1.1) was collected by hand during a rebreather dive at Amber's Arches (21.887, -159.602) at 22.86 m depth off of the island of Kaua‘i and immediately preserved in 95% ethanol. This specimen was deposited at the Bernice Pauahi Bishop Museum (Holly Bollick, holly@bishopmuseum.org, catalogue number: D2772, accession number: 2022.074).

Figure 1.1. *Cirrhipathes* cf. *anguina* LS-2022 taken by Daniel Wagner. Colonies of this wire coral are unbranched and can grow to 2 m or more.

We sequenced the complete mitochondrial genome of *Cirrhipathes* cf. *anguina* LS-2022 (ON653414) using a restriction-site associated DNA sequencing method (ezRAD, Toonen et al., 2013) on the Illumina platform, an approach documented to recover complete mitogenomes for a variety of coral species (Forsman et al., 2017). Sample identification was based on the original species description (Dana 1846) and morphological comparisons with the Antipatharian fauna of Hawai`i, as detailed in Wagner (2015). Genomic DNA was extracted using the E-Z 96 Tissue DNA Kit (Omega Bio-Tek, Norcross, GA) with elution in High-Performance Liquid Chromatography (HPLC) grade water. Extracted gDNA was quantified using the Biotium AccuClear Ultra High Sensitivity dsDNA kit (Biotium, Fremont, CA). The ezRAD libraries were created following the protocol of Knapp et al. (2016). We used the restriction enzyme DpnII (New England Biolabs), and gDNA was size-selected using PCRClean DX (Aline Biosciences, Woburn, MA) beads. As per manufacturer recommendations, DNA fragments of 300-600bp were prepared for sequencing using the Illumina TruSeq® Nano DNA Library Preparation kit.

After passing quality control checks, libraries were sequenced on an Illumina® MiSeq (V3 2x300 bp PE). Trim Galore! (Krueger, 2015) was used to apply quality filters and trim Illumina adapters from sequence reads. Low-quality base calls (Phred score of <20) were trimmed from the ends before the removal of the first 13 bp of the standard Illumina paired-end adapters ('AGATCGGAAGAGC'). The SPAdes (Bankevich et al., 2012) genome assembler generated a 20,518 bp contig.

The contig was circularized, and overlapping ends were trimmed in Geneious Prime 2022.1.1 (https://www.geneioius.com). Protein coding regions were identified via the live annotate feature in Geneious Prime 2022.1.1 (Fig 1.2) based on published antipatharian mitogenomes from *Stichopathes* sp. SCBUCN-8849 (Asorey et al., 2021), *Stichopathes* sp. SCBUCN-8850 (Asorey et al., 2021) and an updated *Stichopathes luetkeni* JX023266, misidentified initially as *Cirrhipathes luetkeni* (Kayal et al., 2013). Gene annotations were performed using MITOS2 (Bernt et al., 2013). This new mitogenome was then compared to complete antipatharian mitochondrial genomes that were >87% identical to *C.* cf. *anguina* LS-2022 (ON653414) to determine the phylogenetic relationships with closely related taxa using *Zoanthus sansibaricus* (Chi and Johansen, 2017) as a known outgroup to these species (79.53%

similar) (Fig 1.3). Annotated regions were first extracted from each mitogenome, aligned separately using default settings in the MAFT v7 plugin (Katoh et al., 2013) for Geneious Prime, and then each annotated region was concatenated into a contiguous sequence following Barret et al. (2020). The relationship among antipatharians was inferred via maximum likelihood, using IQTREE v. 2.0.3 (Nguyen et al., 2015) under the best-fit substitution model, determined by ModelFinder (Kalyaanamoorthy et al., 2017) for 1,000 ultrafast bootstraps (Hoang et al., 2018), as well as the Shimodaira-Hasegawa-like approximate likelihood ratio test (Guindon et al., 2010).

RESULTS

The mitogenome of *Cirrhipathes* cf. *anguina* LS-2022 is 20,452 bp with a base composition of A (29.0%), T (35.9%), C (15.2%), G (19.95%). Like other Hexacorallia, there are 13 protein-coding genes, two rRNA genes (*rnl* and *rns*) and two tRNA genes (*trnM* and *trnW*) plus a cytochrome c oxidase subunit I (*COX1*) intron with embedded homing endonuclease gene (*HEG*), as found in other antipatharian families (Barrett et al. 2020, Fig 2). Read depth ranged from 3 to 46, averaging 22 across the mitogenome. The resulting phylogenetic tree places *Cirrhipathes* cf. *anguina* LS-2022 as sister to the closest BLAST hit *Stichopathes sp.* SCBUCN-8849 (Barrett et al. 2020) in our analysis (Fig 1.3).

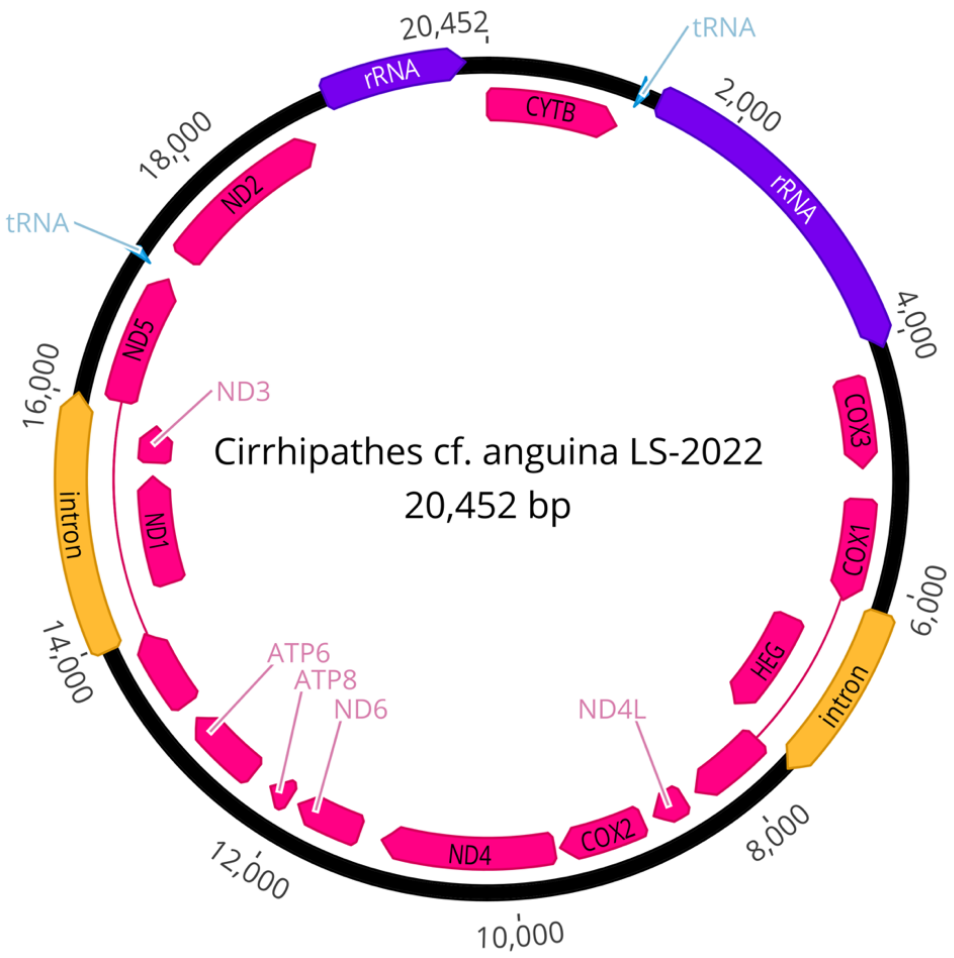

Figure 1.2. Map of the complete mitochondrial genome of *Cirrhipathes* cf. *anguina* LS-2022, drawn by Geneious Prime version 2022.2.2 (https://www.geneious.com).

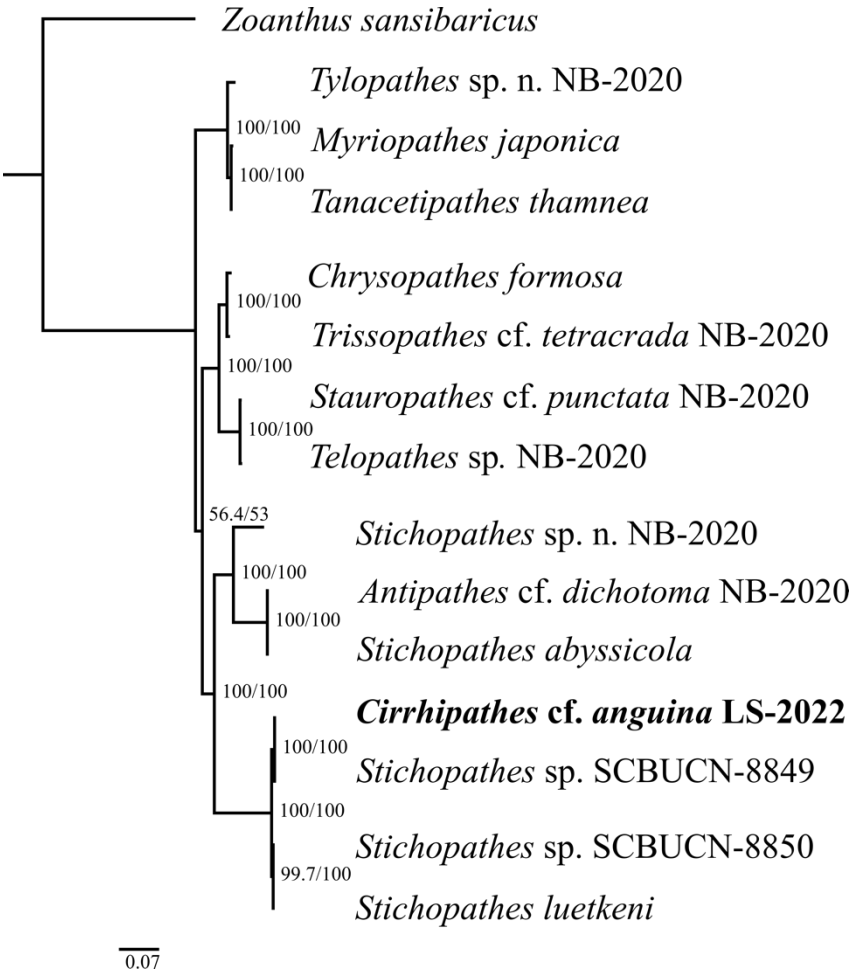

Figure 1.3. Phylogenetic reconstruction of 13 most closely related antipatharian taxa for which complete mitogenomes are currently available (>87% identical to *Cirrhipathes* cf. *anguina* LS-2022). Branch lengths are relative to genetic divergence, and values on each node represent SH-aLRT /ultrafast bootstrap values. Species used include the following: *Stichopathes* sp. SCBUCN-8849 (Asorey et al. 2021), *Stichopathes* sp. SCBUCN-8850 (Asorey et al. 2021), Trissopathes cf. tetracrada NB-2020 (Barrett et al. 2020), *Stichopathes* sp. n. NB-2020 (Barrett et al. 2020), *Tylopathes* sp. n. NB-2020 (Barrett et al. 2020), *Antipathes* cf. *dichotoma* NB-2020 (Barrett et al. 2020), *Stichopathes abyssicola* (Barrett et al. 2020), *Telopathes* sp. NB-2020 (Barrett et al. 2020), *Stauropathes* cf. *punctata* NB-2020 (Barrett et al. 2020), *Chrysopathes formosa* (Brugler and France 2007), *Tanacetipathes thamnea* (Figueroa et al. 2019), *Stichopathes luetkeni* (Kayal et al. 2013), and *Myriopathes japonica* (Kwak et al. 2015).

DISCUSSION

This paper provides the first complete mitogenome sequence from the genus *Cirrhipathes*. It is highly similar (99.97%) to that previously reported for *Stichopathes* sp. (MZ157400, Barrett et al., 2020). Interspecific *Stichopathes* mitogenomes sequenced to date differ by 0.9 – 2.2%, which is roughly the same magnitude of difference by which these species differ from the mitogenomes of *Antipathes* species (Asorey et al., 2021). The *Stichopathes* sequenced by Asorey et al. (2021) and our *Cirrhipathes* sample were collected nearly 8,000 km apart (Rapa Nui and Hawai‘i) and identified morphologically as belonging to different genera. *Cirrhipathes anguina* is a valid name recognized in the World Register of Marine Species, but intergeneric taxa are unlikely to share similar mitogenomes. Interestingly, *ITS1*-based reconstructions place *Stichopathes* sp. SCBUCN-8849 within a clade comprises species within the genus *Cirrhipathes* (Asorey et al., 2021).

This new mitogenome adds to previous phylogenetic work and amplifies the call for additional taxa to be sequenced to support taxonomic revision of the Antipathidae (Bo et al., 2012; Asorey et al., 2021). Phylogenetic reconstructions based on complete mitogenomes are valuable for understanding this group's evolutionary history and taxonomy, which have considerable ecological, cultural, and economic value (Wagner et al., 2012). Additional samples from taxonomically validated *Cirrhipathes* spp. are needed to confirm this sample's taxonomic affinity relative to congeners and to existing *Stichopathes* samples sequenced across the broad geographic range of the group. Regardless of the taxonomic outcome, this study will provide a basis to evaluate the nominal taxonomy of Hawaiian antipatharians, their geographic distribution, and the relationships within this understudied taxonomic group.

LITERATURE CITED

Asorey, C. M., Sellanes, J., Wagner, D., & Easton, E. E. (2021). Complete mitochondrial genomes of two species of *Stichopathes* Brook, 1889 (Hexacorallia: Antipatharia: Antipathidae) from Rapa Nui (Easter Island). *Mitochondrial DNA Part B*, *6*(11), 3226-3228.

Bankevich, A., Nurk, S., Antipov, D., Gurevich, A. A., Dvorkin, M., Kulikov, A. S., ... & Pevzner, P. A. (2012). SPAdes: a new genome assembly algorithm and its applications to single-cell sequencing. *Journal of Computational Biology*, *19*(5), 455-477.

Barrett, N. J., Hogan, R. I., Allcock, A. L., Molodtsova, T., Hopkins, K., Wheeler, A. J., & Yesson, C. (2020). Phylogenetics and mitogenome organization in black corals (Anthozoa: Hexacorallia: Antipatharia): an order-wide survey inferred from complete mitochondrial genomes. *Frontiers in Marine Science*, *7*, 440.

Bernt, M., Donath, A., Jühling, F., Externbrink, F., Florentz, C., Fritzsch, G., Pütz, J., Middendorf, M., & Stadler, P. F. (2013). MITOS: improved de novo metazoan mitochondrial genome annotation. *Molecular Phylogenetics and Evolution*, *69*(2), 313-319.

Bo, M., Bavestrello, G., Barucca, M., Makapedua, D. M., Poliseno, A., Forconi, M., Ettore, O., & Canapa, A. (2012). Morphological and molecular characterization of the problematic whip black coral genus Stichopathes (Hexacorallia: Antipatharia) from Indonesia (North Sulawesi, Celebes Sea). *Zoological Journal of the Linnean Society*, *166*(1), 1-13.

Brugler, M. R., & France, S. C. (2007). The complete mitochondrial genome of the black coral Chrysopathes formosa (Cnidaria: Anthozoa: Antipatharia) supports classification of antipatharians within the subclass Hexacorallia. *Molecular Phylogenetics and Evolution*, *42*(3), 776-788.

Chi, S. I., & Johansen, S. D. (2017). Zoantharian mitochondrial genomes contain unique complex group I introns and highly conserved intergenic regions. Gene, 628, 24-31.

Figueroa, D. F., Hicks, D., & Figueroa, N. J. (2019). The complete mitochondrial genome of *Tanacetipathes thamnea* Warner, 1981 (Antipatharia: Myriopathidae). *Mitochondrial DNA Part B*, 4(2), 4109-4110.

Forsman, Z. H., Knapp, I. S. S., Tisthammer, K., Eaton, D. A. R., Belcaid, M., & Toonen, R. J. (2017). Coral hybridization or phenotypic variation? Genomic data reveal gene flow

between *Porites lobata* and *P. compressa*. *Molecular Phylogenetics and Evolution*, *111*, 132-148.

Hoang, D. T., Chernomor, O., Von Haeseler, A., Minh, B. Q., & Vinh, L. S. (2018). UFBoot2: improving the ultrafast bootstrap approximation. *Molecular Biology and Evolution*, *35*(2), 518-522.

Grigg, R. W. (2001). Status of the black coral fishery in Hawaii, 1998. *Pac. Sci*, *55*, 291-299.

Grigg, R. W. (2004). Harvesting impacts and invasion by an alien species decrease estimates of black coral yield off Maui, Hawai'i. *Pacific Science*, *58*(1), 1-6.

Guindon, S., Dufayard, J. F., Lefort, V., Anisimova, M., Hordijk, W., & Gascuel, O. (2010). New algorithms and methods to estimate maximum-likelihood phylogenies: assessing the performance of PhyML 3.0. *Systematic Biology*, *59*(3), 307-321.

Kalyaanamoorthy, S., Minh, B. Q., Wong, T. K., Von Haeseler, A., & Jermiin, L. S. (2017). ModelFinder: fast model selection for accurate phylogenetic estimates. *Nature Methods*, *14*(6), 587-589.

Katoh, K., & Standley, D. M. (2013). MAFFT multiple sequence alignment software version 7: improvements in performance and usability. *Molecular Biology and Evolution*, *30*(4), 772-780.

Kayal, E., Roure, B., Philippe, H., Collins, A. G., & Lavrov, D. V. (2013). Cnidarian phylogenetic relationships as revealed by mitogenomics. *BMC Evolutionary Biology*, *13*(1), 1-18.

Knapp, I., Puritz, J., Bird, C., Whitney, J., Sudek, M., Forsman, Z., & Toonen, R. J. (2016). ezRAD-an accessible next-generation RAD sequencing protocol suitable for non-model organisms_v3. 2. an accessible next-generation RAD sequencing protocol suitable for non-model organisms_v3.2. https://dx.doi.org/10.17504/protocols.io.e9pbh5n.

Krueger, F. (2015). Trim Galore!: A wrapper around Cutadapt and FastQC to consistently apply adapter and quality trimming to FastQ files, with extra functionality for RRBS data. *Babraham Institute*.

Molodtsova T, Opresko D. 2023. World List of Antipatharia. In: Bánki O et al. *Catalogue of Life Checklist* (ver. 09/2023). [accessed 2023 September 12]. Available at https://doi.org/10.48580/dfpz-3g7.

Nguyen, L. T., Schmidt, H. A., Von Haeseler, A., & Minh, B. Q. (2015). IQ-TREE: a fast and effective stochastic algorithm for estimating maximum-likelihood phylogenies. *Molecular Biology and Evolution*, *32*(1), 268-274.

Toonen, R. J., Puritz, J. B., Forsman, Z. H., Whitney, J. L., Fernandez-Silva, I., Andrews, K. R., & Bird, C. E. (2013). ezRAD: a simplified method for genomic genotyping in non-model organisms. *PeerJ*, *1*, e203.

Wagner, D., Luck, D. G., & Toonen, R. J. (2012). The biology and ecology of black corals (Cnidaria: Anthozoa: Hexacorallia: Antipatharia). *Advances in Marine Biology*, *63*, 67-132.

Wagner, D. (2015). The spatial distribution of shallow-water (< 150 m) black corals (Cnidaria: Antipatharia) in the Hawaiian Archipelago. *Marine Biodiversity Records*, *8*, e54.

CHAPTER 2

UNVEILING THE MYSTERIES OF ʻĒKAHA KŪ MOANA: MITOGENOMIC INSIGHTS REVEAL TAXONOMIC CHALLENGES FOR HAWAIIAN BLACK CORALS

ABSTRACT

We present complete mitochondrial genomes of ten individuals from six antipatharian species (*Antipathes grandis*, *Antipathes griggi*, *Aphanipathes verticillata*, *Cirrhipathes* cf. *anguina*, *Myriopathes ulex* and *Stichopathes* sp.) collected across the Main and Northwestern Hawaiian Islands. In addition to their ecological and economic value, black corals in Hawaiʻi (ʻēkaha kū moana) hold special cultural significance because they are revered as ancestral progenitors from the Kumulipo, the Hawaiian creation story. Mitochondrial genomes varied in size from 17,711 to 20,462 bp, with the Hawaiian Myriopathidae being consistently smaller than members of the other two families. Mitogenome size variation was due primarily to intergenic regions, with the only gene content variation being the presence or absence of a *COX1*-embedded homing endonuclease gene (*HEG*). Otherwise, gene content was highly conserved among ʻēkaha kū moana mitogenomes and all ten contain 13 protein-coding, two rRNA, and two tRNA genes. Phylogenetic reconstructions based on complete mitogenomes support monophyly of the Myriopathidae, but not Aphanipathidae nor Antipathidae. Both the genera *Antipathes* and *Stichopathes* (family Antipathidae) include species that are more divergent from one another than either is to a member of the family Aphanipathidae. Our results are consistent with previous work in emphasizing the need for taxonomic revision.

INTRODUCTION

Antipatharians, commonly known as black corals, are a globally distributed, slow-growing, and long-lived order of hexacoral cnidarians. They occupy a broad bathymetric range (Bo et al., 2012; Wagner et al., 2012; Hitt et al., 2020), with the deepest record observed at 8600 m (Molodstova et al., 2008; Yesson et al., 2017). Their longevity makes them particularly susceptible to anthropogenic perturbances, such as those caused by bottom trawl fishing (Koslow et al., 2001; Sampaio et al., 2012; Wagner et al., 2012). These colonial suspension feeders are characterized by small, non-retractile polyps with six unbranched tentacles and a spiny,

proteinaceous skeleton (Opresko, 1972; France et al., 2007; Molodstova and Budaeva, 2007; Wagner et al., 2012; Wagner, 2015). Antipatharians exhibit diverse growth forms, from unbranched to branched into a bush, fan, feather, or bottle-brush morphology. Their tissues display various colors, including brown, red, orange, pink, yellow, green, white, and grey; all these characters have been proposed to be taxonomically informative in some cases (Wagner et al., 2012).

Antipatharians are ecologically important because they form the primary structural framework of living benthic habitats between 50–200m (Wagner et al., 2012). About 63% of species documented to date are found at depths between 30–150 m (Bo et al., 2019). As ecosystem engineers, they significantly enhance biodiversity by creating a habitat within which various other organisms associate strongly (Criales et al., 1980; Boland and Parish, 2005; Love et al., 2007; Molodstova and Budaeva, 2007; Wagner et al., 2012; Gress and Kaimuddin, 2021; Brickner et al., 2022; Ávila-García et al., 2023; Gonzalez et al., 2023). Numerous cultures across the globe treasure black corals for medicinal purposes, and many prize them for jewelry. The name Antipatharian comes from two Greek words ("*anti*" and "*pathos*") that literally translate to "against disease" (Wagner et al., 2012).

In Hawai‘i, black corals (‘ēkaha kū moana, which translates to "fern of the sea") are of cultural, economic, and ecological importance. The Kumulipo, the Hawaiian creation story consisting of over 2,000 lines, traces the genealogy of Native Hawaiians (Kānaka ‘Ōiwi) back to the origins of the universe. The Kumulipo begins with the emergence of the coral (ko‘a) from darkness and continues through the creation of the Hawaiian Islands, plants, animals, and humans. It is widely believed that ‘ēkaha kū moana symbolizes the ko‘a mentioned in the opening lines of the Kumulipo because ‘ēkaha kū moana are typically found in lightless ocean depths. Kānaka ‘Ōiwi thus hold great reverence for the ko‘a as their ancestral progenitor. This chant embodies the interconnectedness of all things, illustrating the profound relationship between Kānaka ‘Ōiwi and the natural environment, or ‘āina. In addition to its cultural importance, ancient Hawaiians used ‘ēkaha kū moana to remedy lung disease and mouth sores (Kaaiakamanu and Akina, 1922).

Commercially designated as the official gemstone of the State of Hawai‘i, ‘ēkaha kū moana supports a multi-million-dollar fishery employing over 500 individuals in manufacturing and retail statewide (Grigg, 2001). Established in 1958, the fishery concentrated on harvesting three species: *Antipathes griggi* (formerly *A. dichotoma*), *Antipathes grandis*, and *Myriopathes* cf. *ulex* (Opresko, 2009; Wagner et al., 2017). SCUBA divers, serving as the primary suppliers, harvest corals from depths of 40 to 70 meters, primarily within the ‘Au‘au Channel. Additionally, albeit to a lesser extent, divers collect corals off the coasts of Kaua‘i and Hawai‘i (Wagner et al., 2017). Surveys from the ‘90s indicated that *A. griggi*, *A. grandis*, and *Myriopathes* cf. *ulex* comprised 90%, 10%, and 1% of the harvests, respectively (Oishi, 1990). A decade later, in 2001, surveys depicted a decline in the biomass of standing black coral stocks compared to earlier observations (Grigg, 2001; Grigg 2004).

Initially, the existence of a depth refuge was believed; however, recent taxonomic work revealed a new subspecies, *Aphanipathes verticillata mauiensis*, previously misidentified as *A. griggi* (Grigg, 2001; Opresko et al., 2012; Wagner et al., 2017). *A. verticillata mauiensis*, morphologically similar to *A. griggi*, was found in the ‘Au‘au Channel at depths of 88 to 130 meters (Opresko et al., 2012; Wagner et al., 2017). Recent studies on antipatharian depth distributions in the ‘Au‘au Channel demonstrated that species composition at harvest depths consisted of 93% *A. griggi* and 7% *A. grandis*, whereas, at 71–130 meters, the composition changed to 68% *A. grandis*, 25% *A. verticillata*, and 7% *A. griggi* (Wagner et al., 2017). The declines in biomass, recent species distribution elucidation, and taxonomic studies not only suggest potential historical overharvesting but also challenge the concept of a depth refuge. Thus, they underscore the susceptibility of *A. griggi* to prolonged fishing pressure. State and federal regulations have imposed size and catch limits to address sustainability concerns, and researchers continue to study different facets of the biology, ecology, and taxonomy of ‘ēkaha kū moana.

Although ‘ēkaha kū moana are among the best-studied antipatharians in the world (Grigg, 1976; Wagner et al., 2012), identification remains challenging due to the lack of high-quality type specimens, poor initial species descriptions based mainly on preserved specimens, and few distinct morphological characters among taxa (Wagner et al., 2010; Wagner, 2015). For example,

type materials are missing for *Cirrhipathes anguina* and *Myriopathes ulex,* and the original species descriptions are vague (Wagner, 2015). Recent species descriptions have relied predominantly on taxonomic characters such as colony branching pattern, polyp structure, and skeletal spine morphology (Wagner et al., 2010), as well as *in situ* photographs and scanning electron microscopy of skeletal features (Wagner, 2015).

However, plasticity in skeletal traits, both within and across species, dramatically complicates the taxonomy of this order (Bo et al., 2012; Wagner et al., 2012; Opresko et al., 2016). Using a suite of morphometrics, *in situ* observations, and genetic characters, the taxonomy of ʻēkaha kū moana has recently been revised (Opresko, 2009; Wagner et al., 2010; Wagner, 2015). Nonetheless, questions of taxonomic affinity and relationships among black coral taxa abound (Wagner et al. 2010; Bo et al., 2012; Barret et al., 2020; Asorey et al., 2021; Tapia-Guerra et al., 2021), and no study to date has examined the full range of species known to exist in Hawaiʻi, nor used a phylogenomic approach to test species boundaries in these taxonomically challenging corals.

Thus, this chapter seeks to produce the first phylogenomic survey of Hawaiian black corals to resolve species boundaries and relationships among the ʻēkaha kū moana. Here, I generate nine new mitogenomes for this understudied group. I then use these mitogenomes to examine the distinct ʻēkaha kū moana morphotypes known to exist in this region and create phylogenies to determine the relationships among the taxa. I use these data in combination with the previous morphological revision to evaluate the status of Hawaiian black coral taxonomy.

METHODS

Sample Collection

For our phylogenomic investigation, we selected a subsample of 10 individuals representing the full range of observable phenotypes and type material from species within the Bernice Pauahi Bishop Museum collection (Figure 2.1 & Table S2.1). Coral fragments were obtained by hand via rebreather diving or from the manned Hawaiʻi Undersea Research

Laboratory submersibles *Pisces IV* or *V* at depths of 20 to 150 m, where Hawaiian black corals are most common (Kahng et al., 2010; Wagner, 2015). All tissue samples were preserved in 95% ethanol and stored at room temperature until DNA was extracted. These samples include six currently recognized species and distinct ‘ēkaha kū moana morphotypes known to occur in the Hawaiian Archipelago (Wagner 2015).

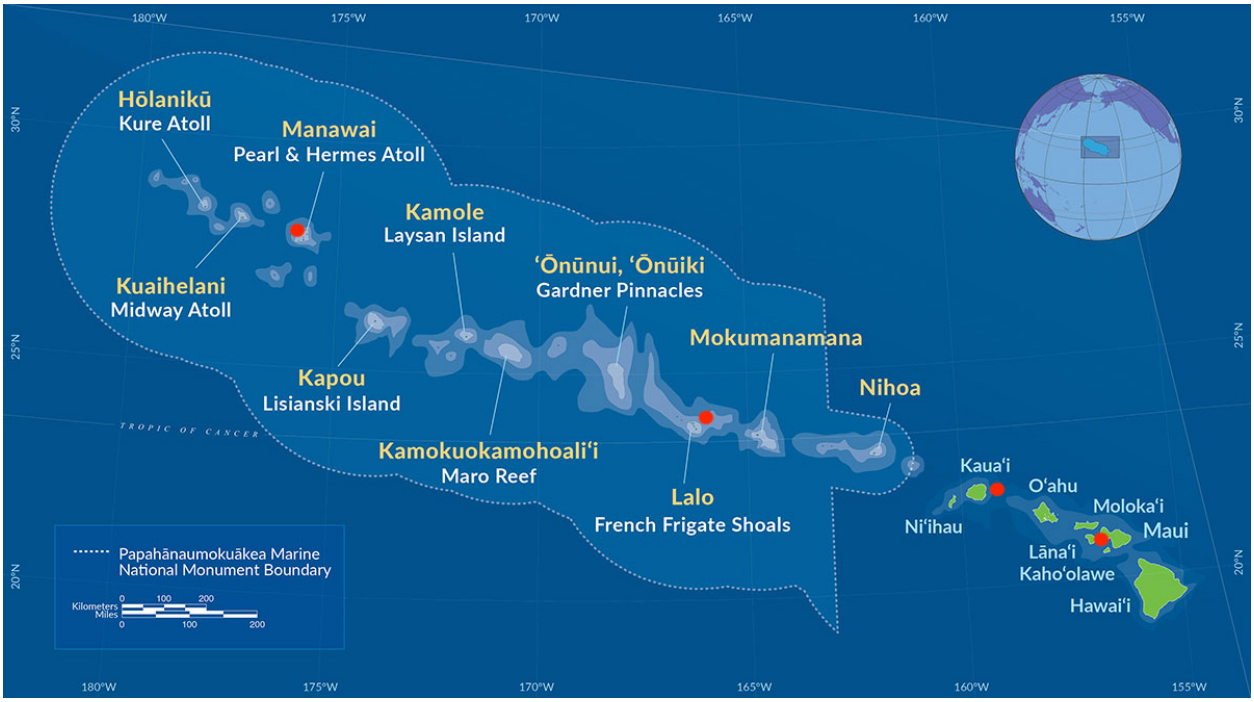

Figure 2.1. Map showing the collection sites of the antipatharians used in this study. See Supplementary Materials, Table S1, for more information. Map courtesy of NOAA Papahānaumokuākea Marine National Monument.

DNA extraction and quantification

Genomic DNA was isolated using a modified protocol for the Omega Bio-Tek (Norcross, GA, USA) E-Z 96 Tissue DNA Kit. We followed the manufacturer protocol but with a two-step elution process. We first conducted an initial rapid elution with 100 µl with HPLC-grade water to selectively eliminate small fragments of degraded DNA. We then performed a second elution using 100 µl of HPLC-grade water, incubated for five minutes at 70°C, to recover the remaining

high molecular weight DNA. We evaluated extraction quality visually by electrophoresis in a 2% agarose gel in TAE buffer. Genomic DNA was stained with GelRed (Biotium, Fremont, CA, USA) and sized relative to 1 kb DNA Hyperladder 1 (New England Biolabs, Ipswich, MA, USA). Samples with a high molecular weight band or a smear with at least half of the total genomic DNA above 2,500 bp were considered acceptable (*sensu* Johnston et al., 2017). We quantified DNA concentrations using the quantification kits of AccuBlue High Sensitivity dsDNA (Biotium, Fremont, CA, USA) or Qubit dsDNA High Sensitivity (Invitrogen, Waltham, MA, USA).

Digestion and library preparation

The ezRAD libraries (Toonen et al., 2013) were generated following Knapp et al. (2016). DNA was digested with the isoschizomers *Mbo*I and *Sau*3AI (New England Biolabs), which recognize 5' GATC cut sites. Post-extraction concentrations were variable, averaging 35.06 ng / µl, so extracts were normalized to the lowest concentration. Digestion with *Mbo*I and *Sau*3AI used 34 µl DNA template at a normalized concentration of 11 ng / µl, 10 µl NEB buffer, 36 µl HPLC grade water, and 2 µl of each *Mbo*I and *Sau*3AI following the manufacturer protocols. Each digestion was incubated in a thermocycler at 37°C for 3 hours, followed by inactivation at 65°C for 20 minutes. Digestions were cleaned using 90 µl of AMPure XP beads (Beckman Coulter, Brea, CA, USA) and resuspended in 33 µl of HPLC-grade water. To visually verify digestion, 3 µl of the bead-cleaned digests were run beside genomic DNA on a 1% agarose gel.

Illumina sequencing

DNA fragments of 300-600 bp were size-selected with Pippen Prep (Sage Science, Beverly, MA, USA), and libraries were prepared with either the Illumina TruSeq Nano (Illumina, San Diego, CA, USA) or Watchmaker DNA Library Preparation (Watchmaker Genomics, Boulder, CO, USA) kits. Following bioanalyzer and qPCR control checks, libraries were sequenced on the Illumina MiSeq (V3 2x300 bp paired-end) at the IIGB Genomics Core facility at UC Riverside or the Advanced Studies in Genomics, Proteomics and Bioinformatics (ASGPB) at the University of Hawai‘i.

Mitochondrial Genome Assembly

TRIM GALORE! v. 0.6.0 (Krueger, 2015) was used to filter and trim low-quality reads and remove Illumina adapters. Ends with Phred <20 were trimmed from the ends before removing the first 13 bp of the standard Illumina paired-end adapters ('AGATCGGAAGAGC'). *De novo* mitogenome assembly was performed with SPAdes v. 3.13.0 (Bankevich et al., 2012). For each *de novo* assembly, a database containing all contigs >10,000 bp was created, and BLAST was used to confirm that only antipatharian sequences were included (See Supplementary code). Contigs with the highest percent identity and query cover to antipatharians were then circularized, and overlapping ends were trimmed in Geneious Prime 2022.1.1 (https://www.geneioius.com). Published antipatharian mitogenomes from *Cirrhipathes* (*Stichopathes*, see below) *luetkeni* (Kayal et al., 2013); *Stichopathes* sp. SCBUCN-8849 (Asorey et al., 2021), *Stichopathes* sp. SCBUCN-8850 (Asorey et al., 2021), *Trissopathes* cf. *tetracrada* NB-2020 (Barrett et al., 2020) and *Chrysopathes formosa* (Brugler and France, 2007) identified protein-coding regions in the live annotate feature in Geneious Prime 2022.1.1. We note here that the taxonomic name *Cirrhipathes luetkeni* (JX023266, Kayal et al., 2013) is invalid as a superseded combination and the proper identification for this sample should be *Stichopathes luetkeni* (WoRMS 2023).

Mitogenome Phylogenetic analyses

Annotated regions of the mitogenome were extracted and aligned separately with the MAFT v7.490 (Katoh and Standley, 2013) plugin in Geneious Prime using the L-INS-I algorithm, a scoring matrix of 200PAM/ k=2, and gap open penalty of 1.53 with an offset value of 0.123. Gene alignments were concatenated, and mitogenomes were compared to published antipatharian mitogenomes to determine the phylogenetic relationships with closely related taxa (*sensu* Barrett et al., 2020). The evolutionary relationships among antipatharians were inferred using a maximum likelihood approach in IQTREE v. 2.0.3 with a partitioned data set (Bui et al., 2020; Chernomor et al., 2016). ModelFinder (Kalyaanamoorthy et al., 2017) was used to determine the best-fit substitution model for gene trees and our partitioned data set. Support for

gene trees and the concatenated data set was evaluated with 1,000 ultrafast bootstrap replicates (Hoang et al., 2018). A Shimodaira-Hasegawa-like approximate likelihood ratio test (Guindon et al., 2010) for branch support was also performed and reported at each node (Figure 2.3).

RESULTS

Mitogenomes

Complete mitochondrial genomes were assembled and annotated for 10 individuals from six species of ʻēkaha kū moana collected across the Main and Northwestern Hawaiian Islands (Figure 2.1 & Table S2.1). These mitogenomes vary in size from 17,711 bp to 20,484 bp (Figures S2.1 to S2.9). Like other Hexacorallia, these mitogenomes contain 13 protein-coding genes (*ATP6*, *ATP8*, *COX1*-3, *CYTB*, *ND1-6*), two rRNA genes (*rnl* and *rns*), and two tRNA genes (*trnM* and *trnW*) (Brugler and France, 2007; Sinniger et al., 2007; Barret et al., 2020; Asorey et al., 2021, Tapia-Guerra et al., 2021). All taxa include a cytochrome c oxidase subunit I (*COX1*) intron and a group 1 intron in NADH dehydrogenase subunit 5 (*ND5*). All but *Aphanipathes verticillata* (#130), *Myriopathes ulex* (#144), and *Myriopathes* cf. *ulex* (#269) contain an embedded homing endonuclease gene (*HEG*, Appendix B), as observed in other antipatharian families (Figure 2.2 & Figures S2.1 to S2.9; Barrett et al., 2020).

Phylogenies

The DNA alignment of the concatenated protein-coding genes was 15, 573 bp long. Although not all gene trees are concordant, maximum likelihood phylogenetic reconstruction based on both *ND4* and *COX1* (Figures S12 & S13) are consistent with the mitogenome phylogeny based on all 13 protein-coding mitochondrial genes when individually aligned and concatenated (Figure 2.3). ModelFinder found TVM+F+G4 to be the best-fit model for our concatenated data set. We find that Aphanipathidae and Antipathidae are closely related, with Myriopathidae as sister to both groups (Figure 2.3). However, there needs to be more support for currently accepted taxonomy because species within *Antipathes*, *Cirrhipathes,* and *Stichopathes* are all polyphyletic (Figure 2.3). Both *Antipathes* and *Stichopathes* include species that are more

divergent from one another than either is to a member of the family Aphanipathidae. Further, there is strong support for Clades B1 and B2 (SH-aLRT= 100 ultrafast bootstrap = 100). Still, these clades each contain members of both Aphanipathidae and Antipathidae, leaving Myriopathidae as the only family that currently appears monophyletic in our dataset of the Hawaiian ʻēkaha kū moana (Figure 2.3).

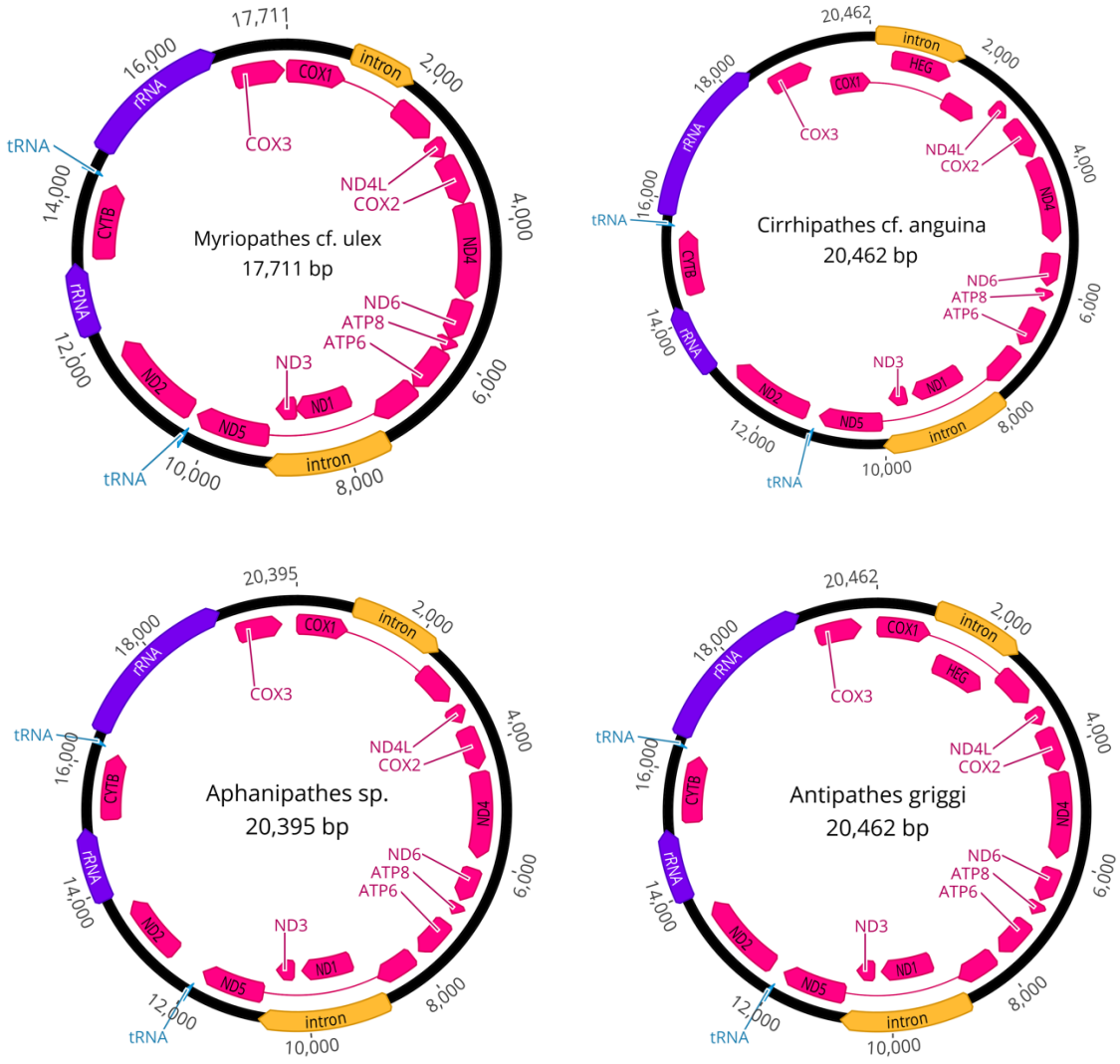

Figure 2.2. Examples of representative antipatharian mitogenomes generated here, highlighting size variation due to intergenic region size and organization. Images drawn by Geneious Prime version 2023.2.1 (https://www.geneious.com).

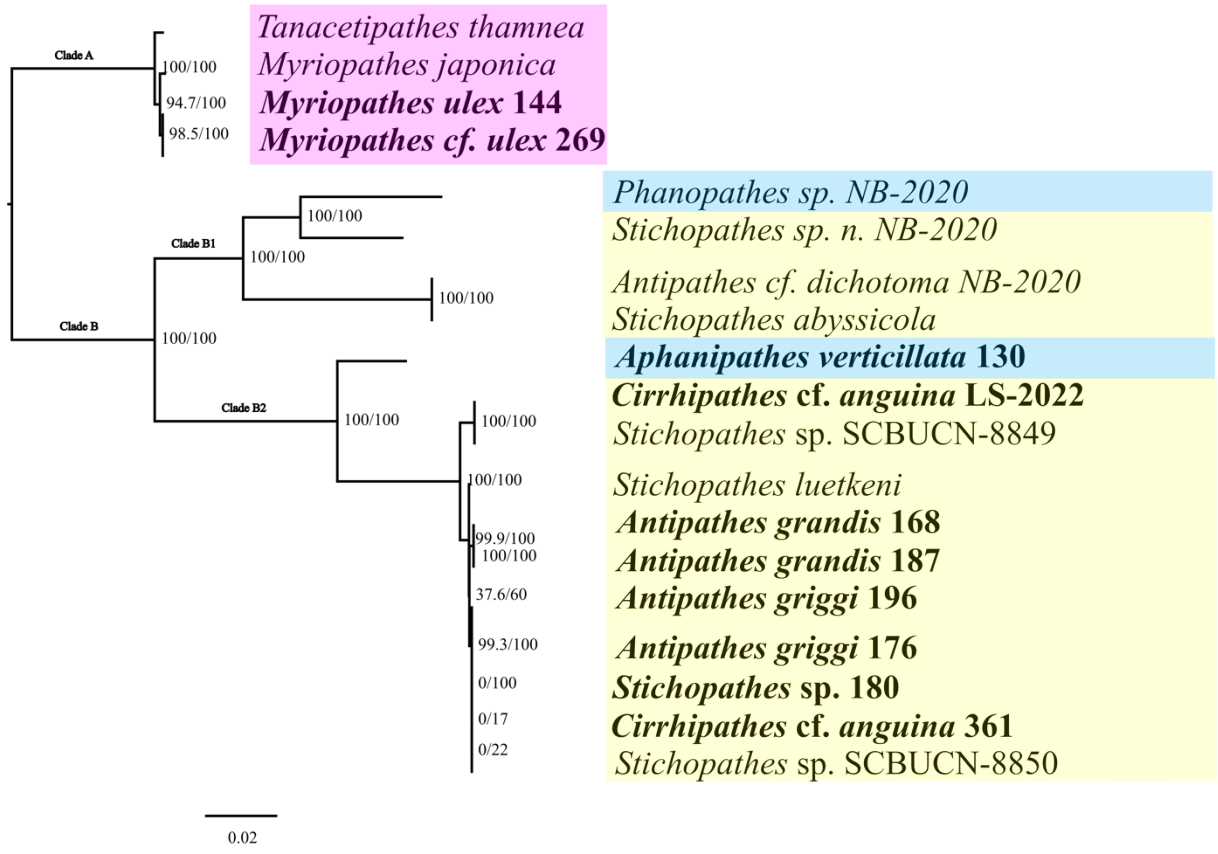

Figure 2.3. Maximum likelihood phylogeny of 19 *Antipatharian* taxa belonging to three families: Myriopathidae (pink), Antipathidae (yellow), and Aphanipathidae (blue). IQ-TREE phylogeny is inferred from 13 individually aligned and concatenated protein-coding mitochondrial genes. The mitogenomes (representing six species of ʻēkaha kū mona) sequenced from Hawaiʻi are bolded (See Supplementary Materials, Table S1 for collection sites). *Antipathes griggi* (#196) is the holotype stored at the Bernice P. Bishop Museum. *Phanopathes* sp. NB-2020, *Stichopathes* sp. n. NB-2020, *Antipathes* cf. *dichotoma* NB-2020, and *Stichopathes abyssicola* were collected in Belgica Mound Province SAC in the NE Atlantic (Irish Margin) (Barrett et al., 2020). *Tanacetipathes thamnea* collected from the Northwestern Gulf of Mexico (Figueroa et al., 2019), *Stichopathes* sp. SCBUCN-8849 and *Stichopathes* sp. SCBUCN-8850 was collected in Rapa Nui (Asorey et al., 2021), and *Myriopathes japonica* was collected in Korea (Kwak et al., 2012, unpublished). The collection location for *Stichopathes luetkeni* (updated from *C. luetkeni*, see text) is unknown (Kayal et al., 2013). Branch lengths are relative to genetic divergence, and values at each node represent SH-aLRT /ultrafast bootstrap values.

DISCUSSION

Here, we provide the first phylogenomic examination of relationships among most of the known ʻēkaha kū moana (Hawaiian black corals). Morphological identification (following Wagner 2015) of these antipatharians places these species into three families (Antipathidae, Aphanipathidae, and Myriopathidae), five genera (*Antipathes, Aphanipathes, Cirrhipathes, Myriopathes,* and *Sticopathes*) and six species (*Antipathes grandis*, *Antipathes griggi*, *Aphanipathes verticillata*., *Myriopathes ulex , Myriopathes* cf. *ulex*, and *Stichopathes* sp.). Because some individuals differ in branching pattern, polyp morphology, thickness of the stem, or color (Table S1), we also include these distinct morphotypes as replicates (e.g., *Myriopathes* cf. *ulex*) to test the hypothesis that they may be cryptic species.

Taxonomy of Antipathidae, Aphanipathidae and Myriopathidae

The family Antipathidae is distinguished by polyps that (1) are approximately 0.5 to 1.0 mm in transverse diameter, (2) are short in the transverse plane, (3) consist of 10 mesenteries (six primary and four secondary), and (4) have two tentacles perpendicular to the branch bearing polyp that are longer than the four tentacles adjacent to the branch bearing polyp (Opresko and Sanchez, 2005; Bo, 2008; Moon and Song, 2008, Wagner, 2015). Although specific genera exhibit clear morphological distinctions, such as the unbranched *Cirrhipathes* (polyps arranged irregularly on all sides of the corallum) and unbranched *Stichopathes*, (polyps arranged in a single row on one side of the corallum) most of the remaining genera are challenging to differentiate. Antipathidae (Ehrenberg 1834) encompasses such diverse genera as *Antipathes* (Pallas, 1766), *Cirrhipathes* (Blainville, 1857), and *Stichopathes* (Brook, 1889). In particular, the genus *Antipathes* is considered a ‘taxonomic dumping ground’ due to the variety and kinds of characters used to distinguish species (Wagner, 2015). Though some species have been reclassified based on colony branching pattern and removed from *Antipathes*, uncertainties remain about taxonomic affinities within this genus (Daly et al., 2007; Bo, 2008; Wagner, 2015; Tapia et al., 2021). Likewise, several genera have been re-classified and removed from Antipathidae, and uncertainty remains about genera still grouped into this family (Daly et al., 2007; Bo, 2008; Wagner, 2015; Tapia et al., 2021).

Corals belonging to the family Aphanipathidae possess obscure polyps (0.7-1.3 mm in transverse diameter), hence its Greek root “aphano” which translates to “invisible” (Opresko, 2004; Wagner, 2015). Further, this family is divided into two subfamilies based on polypar spine development: Aphanipathinae and Acanopathinae (Opresko, 2004). Corals that belong to Aphanipathinae have skeletal spines of similar heights on the side of the corallum where the polyps exist (Opresko, 2004; Wagner, 2015). In contrast, Acanthopathinae present spines directly below the oral opening and on the outer edges of polyps (Opresko, 2004; Wagner, 2015).

Myriopathidae, which comes from the Greek word "myriophylla”, signifying many branches, is named for the numerous branching patterns displayed by the corals belonging to this family (Opresko, 2001; Wagner, 2015). Corals in this family contain polyps with six primary and four secondary mesenteries that are 0.5-1.0 mm in transverse diameter. Corals in the Myriopathidae family have short, rounded tentacles (Opresko, 2001; Wagner, 2015). All corals sequenced in this study were identified following Wagner (2015).

Mitogenome size and structure

We include the first mitogenome sequenced from ‘ēkaha kū moana, *Cirrhipathes* cf. *anguina* LS-2022 (Chapter 1) and add nine additional antipatharian mitogenomes to the 28 published previously. These ten new mitogenomes include the first representation of the genera *Aphanipathes* and *Cirrhipathes* to date. There is considerable disparity in mitogenome size ranging from 17,711 to 20,462 bp (Figure 2.2) due primarily to variation in the length of intergenic regions among taxa. Widespread differences among Hexacorallia in mitogenome size due to intergenic regions are also known from Antipatharia, Zoantharia, Actinaria, and Scleractinia (Barrett et al., 2020; Sinniger et al., 2007). Based on our limited sample size, it appears that Myriopathidae tend to have a consistently smaller mitogenome (17,711bp). Still, with low sample size and only a single representative of Aphanipathidae, it is not possible to say whether mitogenome size is a diagnostic character for ‘ēkaha kū moana, but this remains an intriguing possibility.

In contrast, one notable characteristic of antipatharians and zoantharians that distinguishes them from other Hexacorallia is the general absence of gene rearrangement (Barrett et al., 2020). The mitogenomes of ʻēkaha kū moana displayed a similar arrangement of genes across families (Figure 2.2, Figures S2.1-S2.9) and showed conservation of gene order and content relative to other Antipatharians (Brugler and France, 2007; Kayal et al., 2013; Barrett et al., 2020; Assorey et al., 2021; Tapia-Guerra et al., 2021). Like many other Hexacorallia, two introns are present in all ʻēkaha kū moana species: one within the cytochrome c oxidase subunit I (*COX1*) and another within the NADH dehydrogenase subunit 5 (*ND5*) (Sinniger et al., 2007; Barrett et al., 2020). However, like many orders of Cnidaria (Actinaria, Corallimorpharia, Scleractinia, Zoanthidea, Gorgonacea, Alyconacea, and Hydroida) and the antipatharian families Schizopathidae and Cladiopathidae (Goddard et al., 2006; Barrett et al., 2020), *Aphanipathes verticillata* (#130), *Myriopathes ulex* (#144), and *Myriopathes* cf. *ulex* (#269) lack an embedded homing endonuclease gene (*HEG*, Supplementary Materials). In contrast, *Phanopathes* sp. NB-2020, *Stichopathes* sp. n. NB-2020 and *Antipathes* cf. *dichotoma* NB-2020 all possess an embedded *HEG* despite their intermediate placement on the tree relative to these three Hawaiian samples. The shared presence or absence of an embedded *HEG* among these ʻēkaha kū moana (currently in different families) seems noteworthy, given such high gene conservation across taxa.

Phylogenomics

We investigated single mitochondrial gene trees to determine if there were inconsistencies among loci for phylogenetic inferences (Appendix B). Myriopathidae was used to root these phylogenies because these mitogenomes were most divergent from other species in our data set (<75% pairwise identity and <75% identical sites). All were similar, though not identical, and *ND4* and *COX1* (Figures S2.12 & S2.13) each showed topological concordance with the complete mitogenome phylogeny based on all 13 protein-coding genes. Among all 13 loci, *ND5* was the most variable gene region, with 77.1% pairwise identity and 36.1% identical sites, suggesting that this region would be most informative for future population genetic analyses.

We show that phylogenomic reconstructions based on our mitogenomes place members of *Myriopathes*, *Aphanipathes*, *Cirrhipathes, Stichopathes,* and *Antipathes* into three clades that do not correspond to the families Myriopathidae, Antipathidae, and Aphanipathidae (Figure 2.3). Only Myriopathidae appears monophyletic, with both genera and species within Antipathidae and Aphanipathidae being polyphyletic. Our work is, therefore, consistent with previous reports of polyphyly among these groups based on *ITS1*, *ITS2*, *COX1*, and mitogenomes (Wagner et al., 2010; Bo et al., 2012; Bo et al., 2018; Barret et al., 2020; Asorey et al., 2021; Tapia-Guerra et al., 2021), which appears to be a consistent finding throughout the Antipatharia (Daly et al., 2007; Wagner, 2015).

Overall, this thesis adds ten mitogenomes to the previous 28 global representatives from this understudied group and offers insights into the current taxonomy of ʻēkaha kū moana, their geographic distribution, and their evolutionary relationships. We confirm that *Myriopathes* cf. *ulex* is not genetically distinct from *Myriopathes ulex* and that the family Myriopathidae appears to be monophyletic based on our sampling to date. However, the two *Cirrhipathes* cf. *anguina* included in our study (LS-2022 and 361) are quite divergent from one another and do not appear to be the same species. Given that type materials are missing for *Cirrhipathes anguina* and *Myriopathes ulex*, it is not possible to compare morphologies, and Wagner (2015) advocated the use of cf. for these taxa pending taxonomic revision, including the designation of a neotype. Likewise, both the families Aphanipathidae and Antipathidae are polyphyletic, and the genera *Antipathes*, *Cirrhipathes,* and *Stichopathes* live up to their reputation as taxonomic dumping grounds (Wagner 2015). Both the genera *Antipathes* and *Stichopathes* (family Antipathidae) include species that are more divergent from one another than either is to a member of the family Aphanipathidae (Figure 2.3). Thus, our study highlights the need for a taxonomic overhaul of antipatharians, as suggested by previous authors (Daly et al., 2007; Wagner et al., 2010; Bo et al., 2012; Wagner, 2015; Bo et al., 2018; Barret et al., 2020; Asorey et al., 2021; Tapia-Guerra et al., 2021).

Implications for conservation and management

The family Antipathidae has been described as a taxonomic catch-all following recent phylogenetic reconstructions comparing available morphological and genetic data (Daly et al., 2007; Bo, 2008; Wagner, 2015). Our phylogenetic analysis of mitogenomes underscores the need for a taxonomic overhaul at all levels of biological organization. Differentiating species is critical for understanding population trends in taxa targeted in any fishery. The discovery that there was no depth refuge for the most targeted species, as once believed, raised significant concerns about the long-term sustainability of the ʻēkaha kū moana fishery. Such taxonomic uncertainty undermines efforts to ensure that future generations have access to this precious resource. Declines of *A*. *griggi*, *A*. *grandis* and *A*. *verticillata* also have implications for a wide range of species that rely on the habitat complexity that ʻēkaha kū moana generates at depths of 20 to 130 m in Hawaiʻi. In addition to the ecological and economic impacts, overfishing of ʻēkaha kū moana carries profound cultural importance (evidenced by the Kumulipo), adding to the conservation value of this group. The combined ecological, economic, and cultural value of ʻēkaha kū moana highlight the importance of basic taxonomic work to resolve these species identities, map their distribution within the Hawaiian Archipelago, and understand their population dynamics to ensure future generations have access to this invaluable natural resource.

LITERATURE CITED

Asorey, C. M., Sellanes, J., Wagner, D., & Easton, E. E. (2021). Complete mitochondrial genomes of two species of Stichopathes Brook, 1889 (Hexacorallia: Antipatharia: Antipathidae) from Rapa Nui (Easter Island). *Mitochondrial DNA Part B*, *6*(11), 3226-3228.

Ávila-García, A., Sánchez, C., Huato-Soberanis, L., Borda, E., & Gómez-Gutiérrez, J. (2023). Continuous reproduction causes stable population structure of Antipatharian-associated shrimp *Sandyella tricornuta* (Decapoda: Palaemonidae). *Pacific Science*, 76(4), 397-410.

Bankevich, A., Nurk, S., Antipov, D., Gurevich, A. A., Dvorkin, M., Kulikov, A. S., ... & Pevzner, P. A. (2012). SPAdes: a new genome assembly algorithm and its applications to single-cell sequencing. *Journal of Computational Biology*, *19*(5), 455-477.

Barrett, N. J., Hogan, R. I., Allcock, A. L., Molodtsova, T., Hopkins, K., Wheeler, A. J., & Yesson, C. (2020). Phylogenetics and mitogenome organisation in black corals (Anthozoa: Hexacorallia: Antipatharia): an order-wide survey inferred from complete mitochondrial genomes. *Frontiers in Marine Science*, *7*, 440..

Bo, M. (2008). *Taxonomy and Ecology of Antipatharians*. Ph.D. thesis. Italy: Universita Politenica Delle.

Bo, M., Bavestrello, G., Barucca, M., Makapedua, D. M., Poliseno, A., Forconi, M., ... & Canapa, A. (2012). Morphological and molecular characterization of the problematic whip black coral genus *Stichopathes* (Hexacorallia: Antipatharia) from Indonesia (North Sulawesi, Celebes Sea). *Zoological Journal of the Linnean Society*, *166*(1), 1-13.

Bo, M., Barucca, M., Biscotti, M. A., Brugler, M. R., Canapa, A., Canese, S., ... & Bavestrello, G. (2018). Phylogenetic relationships of Mediterranean black corals (Cnidaria: Anthozoa: Hexacorallia) and implications for classification within the order Antipatharia. *Invertebrate Systematics*, *32*(5), 1102-1110.

Bo, M., Montgomery, A. D., Opresko, D. M., Wagner, D., & Bavestrello, G. (2019). Antipatharians of the mesophotic zone: four case studies. *Mesophotic Coral Ecosystems*, 683-708.

Boland, R. C., & Parrish, F. A. (2005). A description of fish assemblages in the black coral beds off Lahaina, Maui, Hawai‘i. *Pacific Science*, *59*(3), 411-420.

Bui Quang Minh, Heiko A. Schmidt, Olga Chernomor, Dominik Schrempf, Michael D. Woodhams, Arndt von Haeseler, and Robert Lanfear (2020) IQ-TREE 2: New models and efficient methods for phylogenetic inference in the genomic era. Molecular Biology and Evolution, in press. https://doi.org/10.1093/molbev/msaa015

Brickner, I., Koplovitz, G., Simon-Blecher, N., & Achituv, Y. (2022). Lost and found: Totton's *Minyaspis faroni* revived and molecular evidence of paraphyly of *Oxynaspis* and *Minyaspis*. Journal of Natural History, 56(37-40), 1459-1473.

Brook, G. (1889). Report on the Antipatharia collected by H.M.S. Challenger during the years 1873-76. *Report on the Scientific Results of the Voyage of H.M.S. Challenger during the years 1873–76. Zoology.* 32 (part 80): i-iii,1-222, pl. 1-15.

Brugler, M. R., & France, S. C. (2007). The complete mitochondrial genome of the black coral *Chrysopathes formosa* (Cnidaria: Anthozoa: Antipatharia) supports classification of antipatharians within the subclass Hexacorallia. *Molecular Phylogenetics and Evolution*, *42*(3), 776-788.

Chernomor, O., Von Haeseler, A., & Minh, B. Q. (2016). Terrace aware data structure for phylogenomic inference from supermatrices. *Systematic Biology*, *65*(6), 997-1008.

Concepcion, G.T., Kahng, S.E., Crepeau, M.W., Franklin, E.C., Coles, S.L. and Toonen, R.J. (2010). Resolving natural ranges and marine invasions in a globally distributed octocoral (genus *Carijoa*). *Marine Ecology Progress Series* 401: 113-127.

Criales, M. M. (1980). Commensal caridean shrimps of Octocorallia and Antipatharia in Curaçao and Bonaire with description of a new species of *Neopontonides*. *Studies on the Fauna of Curaçao and other Caribbean Islands*, *61*(1), 68-85.

Daly, M., Brugler, M. R., Cartwright, P., Collins, A. G., Dawson, M. N., Fautin, D. G., France, S. C., McFadden, C. S., Opresko, D. M., Rodriguez, E., Romano, S., & Stake, J. (2007). The phylum Cnidaria: A review of phylogenetic patterns and diversity 300 years after Linnaeus. In Z.-Q. Zhang & W. A. Shear (Eds.), *Linnaeus Tercentenary: Progress in Invertebrate Taxonomy* (pp. 127-182). Zootaxa, 1668, 1-766.

Figueroa, D. F., Hicks, D., & Figueroa, N. J. (2019). The complete mitochondrial genome of *Tanacetipathes thamnea* Warner, 1981 (Antipatharia: Myriopathidae). *Mitochondrial DNA Part B*, *4*(2), 4109-4110.

France, S.C., Brugler, M.R., and Opresko, D.M. (2007). Order Antipatharia. In 'The Phylum Cnidaria: a Review of Phylogenetic Patterns and Diversity 300 Years after Linnaeus'. (Eds M.Daly, M.R. Brugler, P.Cartwright, A.G. Collins, M.E. Dawson, et al.) pp. 136-138. *Zootaxa* 1668, 127-182.

Hitt, N. T., Sinclair, D. J., Fallon, S. J., Neil, H. L., Tracey, D. M., Komugabe-Dixson, A., & Marriott, P. (2020). Growth and longevity of New Zealand black corals. *Deep Sea Research Part I: Oceanographic Research Papers*, *162*, 103298.

Hoang, D. T., Chernomor, O., Von Haeseler, A., Minh, B. Q., & Vinh, L. S. (2018). UFBoot2: improving the ultrafast bootstrap approximation. *Molecular Biology and Evolution*, *35*(2), 518-522.

Hourigan TF, Etnoyer PJ, Cairns SD (2017) The State of Deep-Sea Coral and Sponge Ecosystems of the United States. NOAA Technical Memorandum NMFS-OHC-4. Silver Spring, MD. 467 pp.

Goddard, M. R., Leigh, J., Roger, A. J., & Pemberton, A. J. (2006). Invasion and persistence of a selfish gene in the Cnidaria. *PLoS One*, *1*(1), e3.

Gonzalez, B. C., Conde-Vela, V. M., & Osborn, K. J. (2023). Synonymization of two, monotypic black-coral-commensal scale worm genera, *Antipathipolyeunoa pettibone*, 1991 and *Parahololepidella pettibone*, 1969 (Polynoidae, Aphroditiformia). ZooKeys, 1178, 61.

Gress, E., & Kaimuddin, M. (2021). Observations of sea anemones (Hexacorallia: Actiniaria) overgrowing black corals (Hexacorallia: Antipatharia). *Marine Biodiversity*, *51*(3), 45.

Grigg, R. W. (1976). Fishery management of precious and stony corals in Hawaii. UNIHISEAGRANT Technical Report TR-77-03. 48 pp.

Grigg, R. W. (2001). Black coral: History of a sustainable fishery in Hawai'i. *Pacific Science*, *55*(3), 291-299.

Grigg, R. W. (2004). Harvesting impacts and invasion by an alien species decrease estimates of black coral yield off Maui, Hawai'i. *Pacific Science*, *58*(1), 1-6.

Guindon, S., Dufayard, J. F., Lefort, V., Anisimova, M., Hordijk, W., & Gascuel, O. (2010). New algorithms and methods to estimate maximum-likelihood phylogenies: assessing the performance of PhyML 3.0. *Systematic biology*, *59*(3), 307-321.

Johnston, E. C., Forsman, Z. H., Flot, J. F., Schmidt-Roach, S., Pinzón, J. H., Knapp, I. S., & Toonen, R. J. (2017). A genomic glance through the fog of plasticity and diversification in *Pocillopora*. *Scientific Reports*, *7*(1), 5991.

Kaaiakamanu, D.M. & Akina J.K. (1922). Hawaiian Herbs of Medicinal Value: Found Among the Mountains and Elsewhere in the Hawaiian Islands, and Known to the Hawaiians to Possess Curative and Palliative Properties Most Effective in Removing Physical Ailments. Board of Health of the Territory of Hawaii.

Kahng, S. E., & Grigg, R. W. (2005). Impact of an alien octocoral, Carijoa riisei, on black corals in Hawaii. *Coral Reefs*, *24*, 556-562.

Kahng, S. E., Garcia-Sais, J. R., Spalding, H. L., Brokovich, E., Wagner, D., Weil, E., ... & Toonen, R. J. (2010). Community ecology of mesophotic coral reef ecosystems. *Coral Reefs*, *29*, 255-275.

Kalyaanamoorthy S, Minh BQ, Wong TKF, von Haeseler A, Jermiin LS. 2017. ModelFinder: Fast model selection for accurate phylogenetic estimates. *Nature Methods 14*(6):587–589.

Katoh, K., & Standley, D. M. (2013). MAFFT multiple sequence alignment software version 7: improvements in performance and usability. *Molecular Biology and Evolution*, *30*(4), 772-780.

Kayal, E., Roure, B., Philippe, H., Collins, A. G., & Lavrov, D. V. (2013). Cnidarian phylogenetic relationships as revealed by mitogenomics. *BMC Evolutionary Biology*, *13*(1), 1-18.

Knapp, I., Puritz, J., Bird, C., Whitney, J., Sudek, M., Forsman, Z., & Toonen, R. J. (2016). ezRAD-an accessible next-generation RAD sequencing protocol suitable for non-model organisms_v3.2. https://dx.doi.org/10.17504/protocols.io.e9pbh5n.

Koslow, J. A., Gowlett-Holmes, K., Lowry, J. K., O'Hara, T., Poore, G. C. B., & Williams, A. (2001). Seamount benthic macrofauna off southern Tasmania: community structure and impacts of trawling. *Marine Ecology Progress Series*, 213, 111-125.

Krueger, F. (2015). Trim galore. *A wrapper tool around Cutadapt and FastQC to consistently apply quality and adapter trimming to FastQ files*, *516*(517).

Love, M. S., Yoklavich, M. M., Black, B. A., & Andrews, A. H. (2007). Age of black coral (Antipathes dendrochristos) colonies, with notes on associated invertebrate species. *Bulletin of Marine Science*, *80*(2), 391-399.

Molodtsova, T., & Budaeva, N. (2007). Modifications of corallum morphology in black corals as an effect of associated fauna. *Bulletin of Marine Science*, *81*(3), 469-480.

Molodtsova, T., & Opresko, D. 2022. World List of Antipatharia. In: Bánki O et al. *Catalogue of Life Checklist* (ver. 07/2022). [accessed 2022 July 17]. Available at https://doi.org/10.48580/dfpz-3g7.

Molodtsova, T. N., Sanamyan, N. P., & Keller, N. B. (2008). Anthozoa from the northern Mid-Atlantic Ridge and Charlie-Gibbs fracture zone. *Marine Biology Research*, *4*(1-2), 112-130.

Moon, H. W., & Song, J. I. (2008). Taxonomy of black coral family Myriopathidae (Anthozoa: Antipatharia) from Korea. *Animal Systematics, Evolution and Diversity*, *24*(3), 251-263.

Oishi, F. (1990). Black coral harvesting and marketing activities in Hawaii-1990. Division of Aquatic Resources Report, Department of Land and Natural Resources, State of Hawai'i.

Opresko, D. M. (2001). Revision of the antipatharia (Cnidaria: Anthozoa). Part I. Establishment of a new family, Myriopathidae. *Zoologische Mededelingen*, *75*, 343-370.

Opresko, D. M. (2004). Revision of the Antipatharia (Cnidaria: Anthozoa). Part IV. *Zoologische Mededelingen*, *78*, 209-240.

Opresko, D. M. (2009). A new name for the Hawaiian Antipatharian coral formerly known as *Antipathes dichotoma* (Cnidaria: Anthozoa: Antipatharia) *Pacific Science*, *63*(2), 277-291.

Opresko, D. M. (1972). Biological results of the University of Miami Deep-Sea Expeditions. 97. Redescriptions and reevaluations of the antipatharians described by LF de Pourtales. *Bulletin of Marine Science*, *22*(4), 950-1017.

Opresko, D.M., Nuttall, M. F. & Hickerson, E. L. (2016). Black corals of the Flower Garden Banks National Marine Sanctuary. *Gulf of Mexico Science* 33,1.

Opresko, D. M., & Sanchez, J. A. (2005). Caribbean shallow-water black corals (Cnidaria: Anthozoa: Antipatharia). *Caribbean Journal of Science*. 41(3), 492-507.

Opresko, D. M., Wagner, D., Montgomery, A. D., & Brugler, M. R. (2012). Discovery of Aphanipathes verticillata (Cnidaria: Anthozoa: Antipatharia) in the Hawaiian Islands. *Zootaxa*, *3348*(1), 24-39.

Sampaio, I., Braga-Henriques, A., Pham, C., Ocaña, O., De Matos, V., Morato, T., & Porteiro, F. M. (2012). Cold-water corals landed by bottom longline fisheries in the Azores (north-eastern Atlantic). *Journal of the Marine Biological Association of the United Kingdom*, 92(7), 1547-1555.

Sinniger, Frédéric, Pierre Chevaldonné, and J. Pawlowski. (2007). Mitochondrial genome of *Savalia savaglia* (Cnidaria, Hexacorallia) and early metazoan phylogeny. *Journal of Molecular Evolution* 64 (2007): 196-203.

Tapia-Guerra, J. M., Asorey, C. M., Easton, E. E., Wagner, D., Gorny, M., & Sellanes, J. (2021). First ecological characterization of Whip Black Coral assemblages (Hexacorallia: Antipatharia) in the Easter Island Ecoregion, Southeastern Pacific. *Frontiers in Marine Science*, *8*, 755898.

Toonen, R. J., Puritz, J. B., Forsman, Z. H., Whitney, J. L., Fernandez-Silva, I., Andrews, K. R., & Bird, C. E. (2013). ezRAD: a simplified method for genomic genotyping in non-model organisms. *PeerJ*, *1*, e203.

Yesson, C., Bedford, F., Rogers, A. D., & Taylor, M. L. (2017). The global distribution of deep-water Antipatharia habitat. *Deep Sea Research Part II: Topical Studies in Oceanography*, *145*, 79-86.

Wagner, D., Brugler, M. R., Opresko, D. M., France, S. C., Montgomery, A. D., & Toonen, R. J. (2010). Using morphometrics, in situ observations and genetic characters to distinguish among commercially valuable Hawaiian black coral species; a redescription of Antipathes grandis Verrill, 1928 (Antipatharia: Antipathidae). *Invertebrate Systematics*, *24*(3), 271-290.

Wagner, D., Luck, D. G., & Toonen, R. J. (2012). The biology and ecology of black corals (Cnidaria: Anthozoa: Hexacorallia: Antipatharia). *Advances in Marine Biology*, *63*, 67-132.

Wagner, D. (2015). The spatial distribution of shallow-water (< 150 m) black corals (Cnidaria: Antipatharia) in the Hawaiian Archipelago. *Marine Biodiversity Records*, *8*, e54.

Wagner, D., Opresko, D.M., Montgomery, A.D., & Parrish, F. A. (2017). An update on recent research and management of Hawaiian black corals. In T. F. Hourigan, P. J. Etnoyer, & S. D. Cairns (Eds.), *The state of deep-sea coral and sponge ecosystems of the United States* (pp. 157-170). *NOAA Technical Memorandum NMFS-OHC-4*. Silver Spring, MD.

WoRMS (2023). *Cirrhipathes lutkeni* (Brook, 1889). Accessed at: https://www.marinespecies.org/aphia.php?p=taxdetails&id=1564697 on 2023-11-01

Table S2.1. ʻĒkaha kū moana (Hawaiian Black Coral) samples used in this study. *Antipathes griggi* #196 represents type material stored at the Bernice Pauahi Bishop Museum (BPBM).

Species name	ID	Location	Depth (m)	Comment
Antipathes grandis	168	Maui	100	
Antipathes grandis	187	Maui	102	*A. grandis* w/red polyps
Antipathes griggi	176	Kauai	23	*A. griggi* w/thick polyps
Antipathes griggi	196	Maui	93	Type: BPBM-D1879
Aphanipathes verticillata	130	Maui	111	
Cirrhipathes cf. *anguina*	361	Lalo	30	
Myriopathes ulex	144	Maui	96	
Myriopathes cf. *ulex*	269	Manawai	61	
Stichopathes sp.	180	Kauai	23	

Table S2.2. Annotations of *Antipathes grandis* (#168)

Name	Type	Start	End	Length	Transferred From	Transferred Similarity
COX1	gene	1 2373	894 3701	1593	*Stichopathes* sp. SCBUCN-8850	99.74%
intron	intron	895	2372	1478	*Stichopathes* sp. SCBUCN-8850	99.66%
HEG	gene	1205	2266	1062	*Stichopathes luetkeni*	99.91%
ND4L	gene	3220	3519	300	*Stichopathes* sp. SCBUCN-8850	100.00%
COX2	gene	3627	4376	750	*Stichopathes* sp. SCBUCN-8850	99.87%
ND4	gene	4433	5935	1503	*Stichopathes* sp. SCBUCN-8850	100.00%
ND6	gene	6141	6731	591	*Stichopathes* sp. SCBUCN-8850	99.83%
ATP8	gene	6806	7018	213	*Stichopathes* sp. SCBUCN-8850	99.53%
ATP6	gene	7192	7890	699	*Stichopathes* sp. SCBUCN-8850	99.86%
ND5	gene	8029 10811	8748 11941	1851	*Stichopathes* sp. SCBUCN-8850	100.00%
intron	intron	8749	10810	2062	*Stichopathes* sp. SCBUCN-8850	99.66%
ND1	gene	9099	10148	1050	n/a	n/a
ND3	gene	10286	10642	357	n/a	n/a
tRNA	tRNA	11986	12055	70	*Stichopathes* sp. SCBUCN-8850	100%
ND2	gene	12175	13692	1518	*Stichopathes* sp. SCBUCN-8850	99.80%
rRNA	rRNA	13922	15070	1149	*Stichopathes* sp. SCBUCN-8850	99.91%
CYTB	gene	15176	16318	1143	*Stichopathes* sp. SCBUCN-8850	99.83%
tRNA	tRNA	16395	16465	71	*Stichopathes* sp. SCBUCN-8850	100.00%
rRNA	rRNA	16570	19232	2663	*Stichopathes* sp. SCBUCN-8850	99.81%
COX3	gene	19400	20188	789	*Stichopathes* sp. SCBUCN-8850	99.75%

Table S2.3. Annotations of *Antipathes grandis* (#187)

Name	Type	Start	End	Length	Transferred From	Transferred Similarity
COX1	gene	1 2373	894 3071	1593	*Stichopathes* sp. SCBUCN-8850	99.74%
intron	intron	895	2372	1478	*Stichopathes* sp. SCBUCN-8850	99.66%
HEG	gene	1205	2266	1062	*Stichopathes luetkeni*	99.91%
ND4L	gene	3220	3519	300	*Stichopathes luetkeni*	100.00%
COX2	gene	3627	4376	750	*Stichopathes luetkeni*	99.87%
ND4	gene	4433	5935	1503	*Stichopathes* sp. SCBUCN-8850	100.00%
ND6	gene	6141	6731	591	*Stichopathes* sp. SCBUCN-8850	99.83%
ATP8	gene	6806	7018	213	*Stichopathes luetkeni*	99.53%
ATP6	gene	7192	7890	699	*Stichopathes* sp. SCBUCN-8850	99.86%
ND5	gene	8029 10811	8748 11941	1851	*Stichopathes luetkeni*	99.72%
intron	intron	8749	10810	2062	*Stichopathes* sp. SCBUCN-8850	99.66%
ND1	gene	9099	10148	1050	*Stichopathes luetkeni*	100.00%
ND3	gene	10286	10642	357	*Stichopathes luetkeni*	100.00%
tRNA	tRNA	11986	12055	70	*Stichopathes* sp. SCBUCN-8850	100.00%
ND2	gene	12175	13692	1518	*Stichopathes* sp. SCBUCN-8850	99.80%
rRNA	rRNA	13922	15070	1149	*Stichopathes luetkeni*	99.91%
CYTB	gene	15176	16318	1143	*Stichopathes luetkeni*	99.83%
tRNA	tRNA	16395	16465	71	*Stichopathes luetkeni*	100.00%
rRNA	rRNA	16570	19232	2663	*Stichopathes* sp. SCBUCN-8850	99.81%
COX3	gene	19400	20188	789	*Stichopathes luetkeni*	99.75%

Table S2.4. Annotations of *Antipathes griggi* (#176)

Name	Type	Start	End	Length	Transferred From	Transferred Similarity
COX1	gene	1 2370	894 3068	1593	*Stichopathes* sp. SCBUCN-8850	99.90%
intron	intron	895	2369	1475	*Stichopathes* sp. SCBUCN-8850	99.80%
HEG	gene	1202	2263	1062	*Stichopathes* sp. SCBUCN-8850	100.00%
ND4L	gene	3217	3516	300	*Stichopathes* sp. SCBUCN-8850	100.00%
COX2	gene	3624	4373	750	*Stichopathes* sp. SCBUCN-8850	100.00%
ND4	gene	4430	5932	1503	*Stichopathes* sp. SCBUCN-8850	100.00%
ND6	gene	6138	6728	591	*Stichopathes* sp. SCBUCN-8850	100.00%
ATP8	gene	6803	7015	213	*Stichopathes* sp. SCBUCN-8850	100.00%
ATP6	gene	7189	7887	699	*Stichopathes* sp. SCBUCN-8850	100.00%
ND5	gene	8026 10808	8745 11938	1851	n/a	n/a
intron	intron	8746	10807	2062	*Stichopathes* sp. SCBUCN-8850	99.95%
ND1	gene	9096	10145	1050	*Stichopathes* sp. SCBUCN-8850	100.00%
ND3	gene	10283	10639	357	*Stichopathes* sp. SCBUCN-8850	100.00%
tRNA	tRNA	11983	12052	70	*Stichopathes* sp. SCBUCN-8850	100.00%
ND2	gene	12172	13689	1518	*Stichopathes* sp. SCBUCN-8850	100.00%
rRNA	rRNA	13919	15067	1149	*Stichopathes* sp. SCBUCN-8850	100.00%
CYTB	gene	15173	16315	1143	*Stichopathes* sp. SCBUCN-8850	100.00%
tRNA	tRNA	16392	16462	71	*Stichopathes* sp. SCBUCN-8850	100.00%
rRNA	rRNA	16567	19229	2663	*Stichopathes* sp. SCBUCN-8850	100.00%
COX3	gene	19396	20184	789	*Stichopathes* sp. SCBUCN-8850	100.00%

Table S2.5. Annoations of *Antipathes griggi* (#196)

Name	Type	Start	End	Length	Transferred From	Transferred Similarity
COX1	gene	1 2373	928 3071	1627	*Stichopathes* sp. SCBUCN-8850	100.00%
COX3	gene	19398	20186	789	*Stichopathes* sp. SCBUCN-8850	100.00%
rRNA	rRNA	16569	19231	2663	*Stichopathes* sp. SCBUCN-8850	100.00%
tRNA	tRNA	16394	16464	71	*Stichopathes* sp. SCBUCN-8850	100.00%
CYTB	gene	15175	16317	1143	*Stichopathes* sp. SCBUCN-8850	100.00%
rRNA	rRNA	13921	15069	1149	*Stichopathes* sp. SCBUCN-8850	100.00%
ND2	gene	12174	13691	1518	*Stichopathes* sp. SCBUCN-8850	100.00%
tRNA	tRNA	11985	12054	70	*Stichopathes* sp. SCBUCN-8850	100.00%
ND3	gene	10286	10642	357	*Stichopathes* sp. SCBUCN-8850	100.00%
ND1	gene	9099	10148	1050	*Stichopathes* sp. SCBUCN-8850	100.00%
intron	intron	8749	10810	2062	*Stichopathes* sp. SCBUCN-8850	99.90%
ND5	gene	8029 10811	8748 11941	1851	n/a	n/a
ATP6	gene	7192	7890	699	*Stichopathes* sp. SCBUCN-8850	100.00%
ATP8	gene	6806	7018	213	*Stichopathes* sp. SCBUCN-8850	100.00%
ND6	gene	6141	6731	591	*Stichopathes* sp. SCBUCN-8850	100.00%
ND4	gene	4433	5935	1503	*Stichopathes* sp. SCBUCN-8850	100.00%
COX2	gene	3627	4376	750	*Stichopathes* sp. SCBUCN-8850	100.00%
ND4L	gene	3220	3519	300	*Stichopathes* sp. SCBUCN-8850	100.00%
HEG	gene	1205	2266	1062	*Stichopathes* sp. SCBUCN-8850	100.00%
intron	intron	929	2372	1444	*Stichopathes* sp. SCBUCN-8850	100.00%

Table S2.6. Annotations of *Aphanipathes verticillata* (#130)

Name	Type	Start	End	Length	Transferred From	Transferred Similarity
COX1	gene	1 2371	894 3069	1593	n/a	n/a
intron	intron	895	2370	1476	n/a	n/a
ND4L	gene	3219	3506	288	*Stichopathes* sp. SCBUCN-8850	95.67%
COX2	gene	3626	4375	750	*Stichopathes* sp. SCBUCN-8849	96.13%
ND4	gene	4432	5934	1503	*Stichopathes* sp. SCBUCN-8850	95.34%
ND6	gene	6138	6728	591	*Stichopathes* sp. SCBUCN-8849	95.09%
ATP8	gene	6805	7017	213	*Stichopathes* sp. SCBUCN-8849 & *Stichopathes* sp. SCBUCN-8850	96.71%
ATP6	gene	7184	7882	699	*Stichopathes* sp. SCBUCN-8850	93.06%
ND5	gene	8016 10777	8735 11907	1851	n/a	n/a
intron	intron	8736	10776	2041	n/a	n/a
ND1	gene	9070	10096	1027	*Stichopathes* sp. SCBUCN-8850	98.00%
ND3	gene	10252	10608	357	*Stichopathes* sp. SCBUCN-8850	96.64%
tRNA	tRNA	11947	12016	70	*Stichopathes* sp. SCBUCN-8850	100.00%
ND2	gene	12499	13644	1146	*Chrysopathes formosa*	90.84%
rRNA	rRNA	13874	15024	1151	Stichopathes sp. SCBUCN-8849	96.79%
CYTB	gene	15132	16274	1143	*Stichopathes* sp. SCBUCN-8850	94.93%
tRNA	tRNA	16352	16422	71	*Trissopathes* cf. *tetracrada* NB-202	97.18%
rRNA	rRNA	16539	19180	2642	*Stichopathes* sp. SCBUCN-8850	92.59%
COX3	gene	19348	20136	789	*Stichopathes* sp. SCBUCN-8850	94.80%

Table S2.7. Annotations of *Cirrhipathes* cf. *anguina* (#361)

Name	Type	Start	End	Length	Transferred From	Transferred Similarity
intron	intron	94	1571	1478	*Stichopathes* sp. SCBUCN-8850	100.00%
HEG	gene	404	1465	1062	*Stichopathes* sp. SCBUCN-8850	100.00%
COX1	gene	19662 1572	20462 2270	1500	*Stichopathes* sp. SCBUCN-8850	99.90%
ND4L	gene	2419	2718	300	*Stichopathes* sp. SCBUCN-8850	100.00%
COX2	gene	2826	3575	750	*Stichopathes* sp. SCBUCN-8850	100.00%
ND4	gene	3632	5134	1503	*Stichopathes* sp. SCBUCN-8850	100.00%
ND6	gene	5340	5930	591	*Stichopathes* sp. SCBUCN-8850	100.00%
ATP8	gene	6005	6217	213	*Stichopathes* sp. SCBUCN-8850	100.00%
ATP6	gene	6391	7089	699	*Stichopathes* sp. SCBUCN-8850	100.00%
ND5	gene	7228 10010	7947 11140	1851	n/a	n/a
intron	intron	7948	10009	2062	*Stichopathes* sp. SCBUCN-8850	99.90%
ND1	gene	8298	9347	1050	*Stichopathes* sp. SCBUCN-8850	100.00%
ND3	gene	9485	9841	357	*Stichopathes* sp. SCBUCN-8850	100.00%
tRNA	tRNA	11184	11253	70	*Stichopathes* sp. SCBUCN-8850	100.00%
ND2	gene	11373	12890	1518	*Stichopathes* sp. SCBUCN-8850	100.00%
rRNA	rRNA	13120	14268	1149	*Stichopathes* sp. SCBUCN-8850	100.00%
CYTB	gene	14374	15516	1143	*Stichopathes* sp. SCBUCN-8850	100.00%
tRNA	tRNA	15593	15663	71	*Stichopathes* sp. SCBUCN-8850	100.00%
rRNA	rRNA	15768	18430	2663	*Stichopathes* sp. SCBUCN-8850	100.00%
COX3	gene	18597	19385	789	*Stichopathes* sp. SCBUCN-8850	100.00%

Table S2.8. Annotations of *Stichopathes* sp. (#180)

Name	Type	Start	End	Length	Transferred From	Transferred Similarity
COX1	gene	1 2370	894 3068	1593	*Stichopathes* sp. SCBUCN-8850	100.00%
intron	intron	895	2369	1475	*Stichopathes* sp. SCBUCN-8850	99.80%
HEG	gene	1202	2263	1062	*Stichopathes* sp. SCBUCN-8850	100.00%
ND4L	gene	3217	3516	300	*Stichopathes* sp. SCBUCN-8850	100.00%
COX2	gene	3624	4373	750	*Stichopathes* sp. SCBUCN-8850	100.00%
ND4	gene	4430	5932	1503	*Stichopathes* sp. SCBUCN-8850	100.00%
ND6	gene	6138	6728	591	*Stichopathes* sp. SCBUCN-8850	100.00%
ATP8	gene	6803	7015	213	*Stichopathes* sp. SCBUCN-8850	100.00%
ATP6	gene	7189	7887	699	*Stichopathes* sp. SCBUCN-8850	100.00%
ND5	gene	8026 10809	8745 11939	1851	n/a	n/a
intron	intron	8746	10808	2063	*Stichopathes* sp. SCBUCN-8850	99.90%
ND1	gene	9096	10146	1051	*Stichopathes* sp. SCBUCN-8850	99.90%
ND3	gene	10284	10640	357	*Stichopathes* sp. SCBUCN-8850	100.00%
tRNA	tRNA	11983	12052	70	*Stichopathes* sp. SCBUCN-8850	100.00%
ND2	gene	12172	13689	1518	*Stichopathes* sp. SCBUCN-8850	100.00%
rRNA	rRNA	13919	15067	1149	*Stichopathes* sp. SCBUCN-8850	100.00%
CYTB	gene	15173	16315	1143	*Stichopathes* sp. SCBUCN-8850	100.00%
tRNA	tRNA	16392	16462	71	*Stichopathes* sp. SCBUCN-8850	100.00%
rRNA	rRNA	16567	19229	2663	*Stichopathes* sp. SCBUCN-8850	100.00%
COX3	gene	19396	20184	789	*Stichopathes* sp. SCBUCN-8850	100.00%

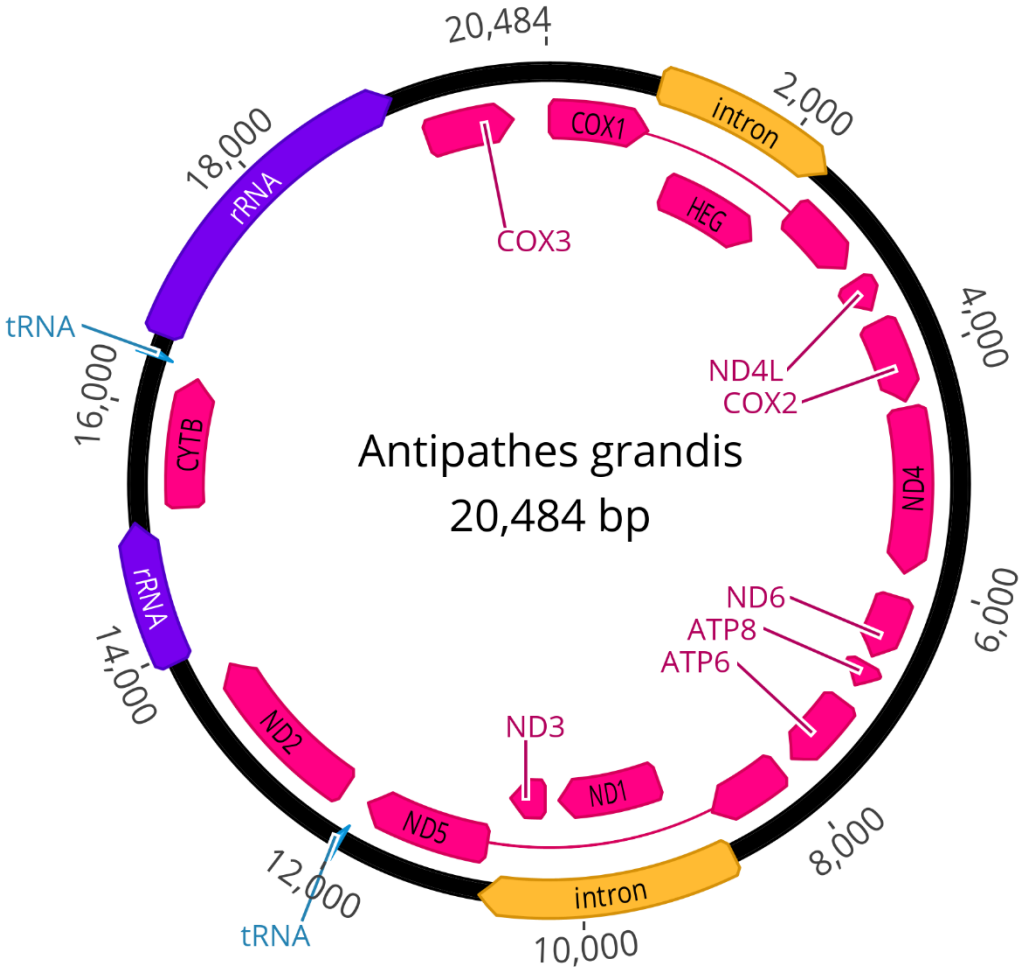

Figure S2.1. Map of the complete mitochondrial genome of *Antipathes grandis* (#168), drawn by Geneious Prime version 2023.2.1 (https://www.geneious.com).

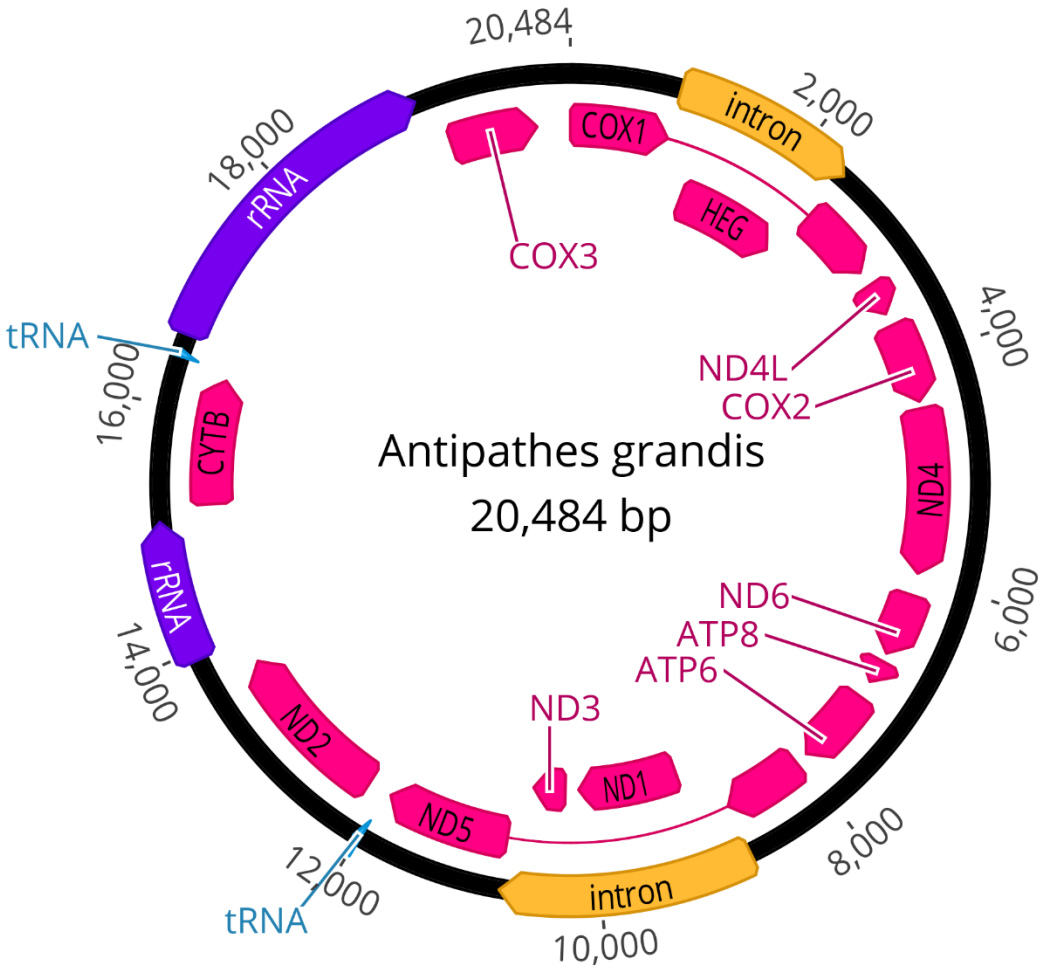

Figure S2.2. Map of the complete mitochondrial genome of *Antipathes grandis* (#187), drawn by Geneious Prime version 2023.2.1 (https://www.geneious.com).

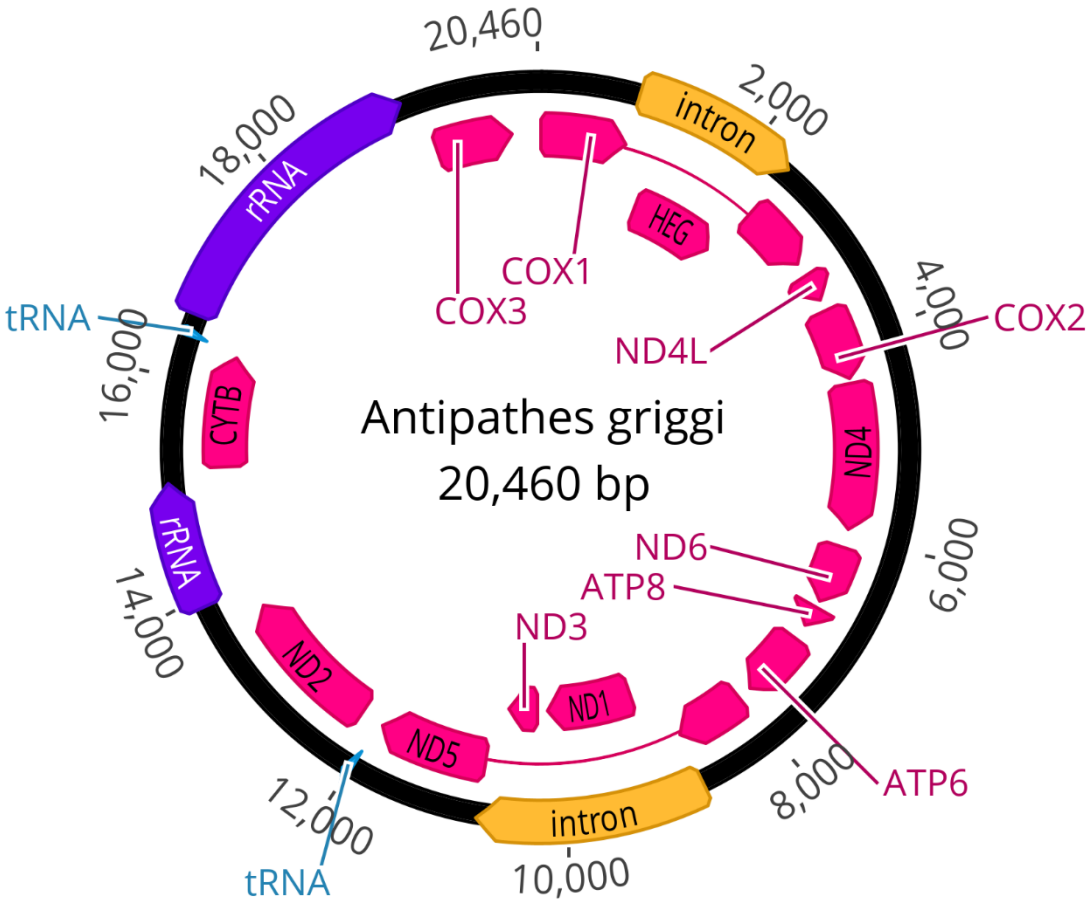

Figure S2.3. Map of the complete mitochondrial genome of *Antipathes griggi* (#176), drawn by Geneious Prime version 2023.2.1 (https://www.geneious.com).

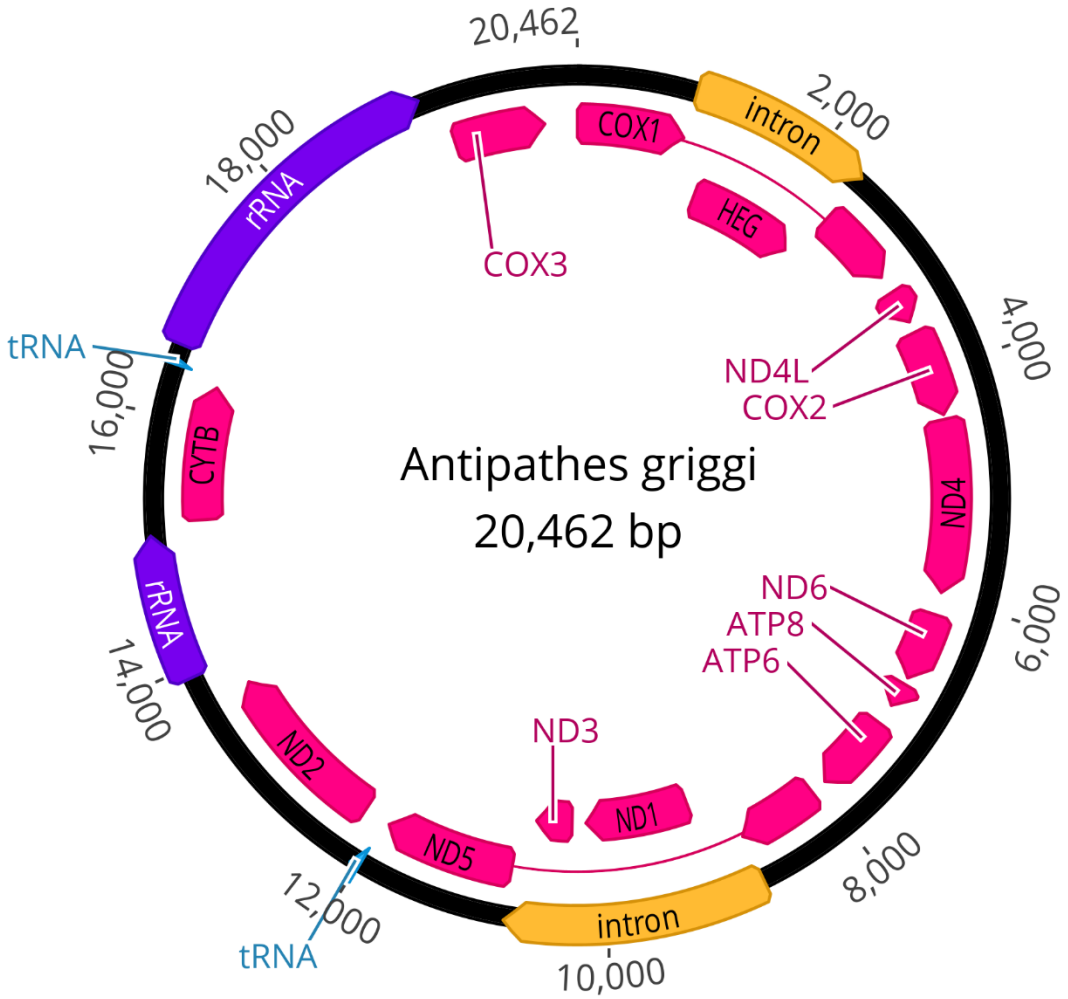

Figure S2.4. Map of the complete mitochondrial genome of *Antipathes griggi* (#196), drawn by Geneious Prime version 2023.2.1 (https://www.geneious.com).

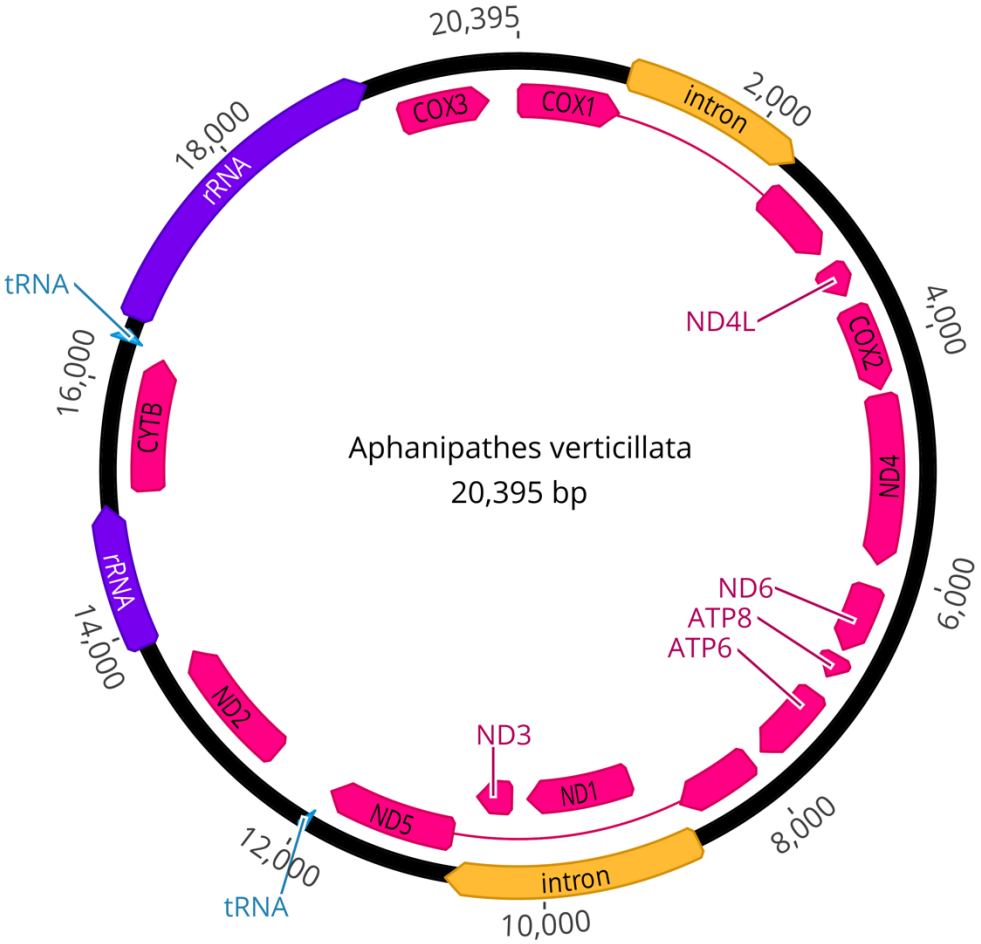

Figure S2.5. Map of the complete mitochondrial genome of *Aphanipathes verticillata* (#130), drawn by Geneious Prime version 2023.2.1 (https://www.geneious.com).

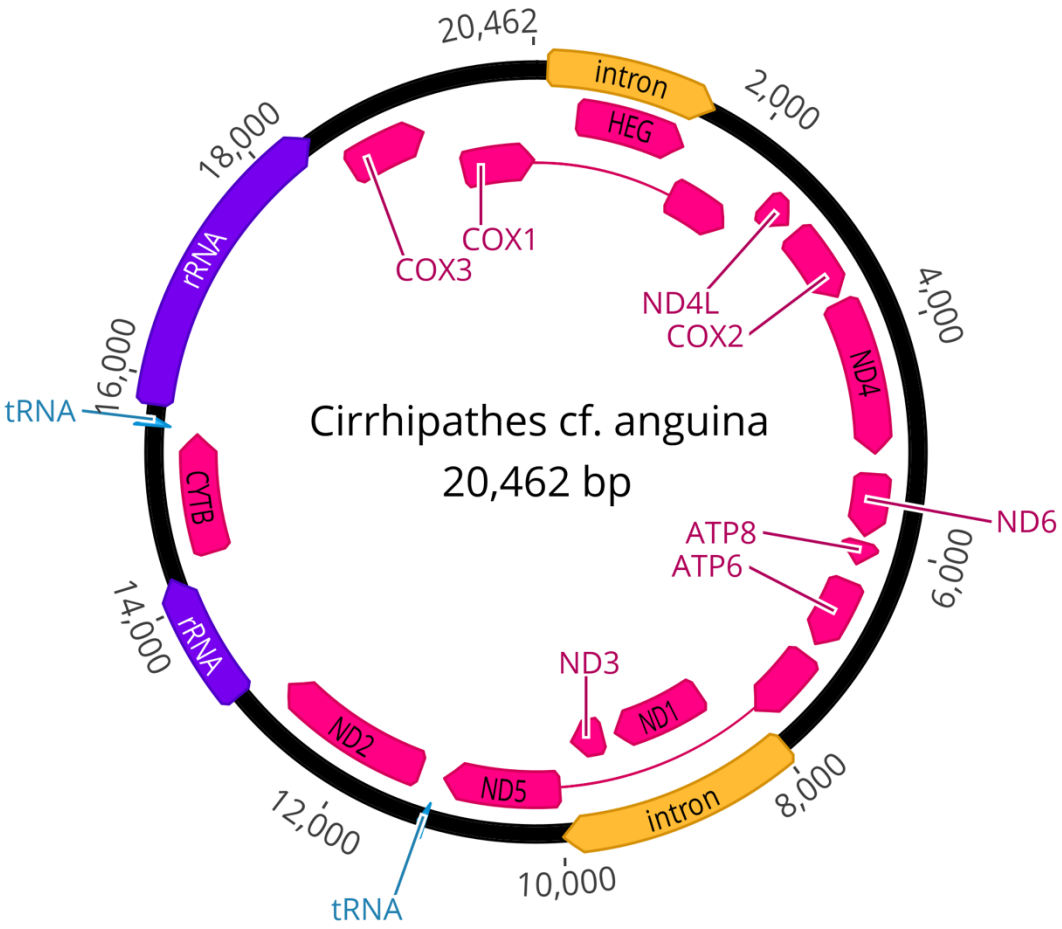

Figure S2.6. Map of the complete mitochondrial genome of *Cirrhipathes cf. anguina* (#361), drawn by Geneious Prime version 2023.2.1 (https://www.geneious.com).

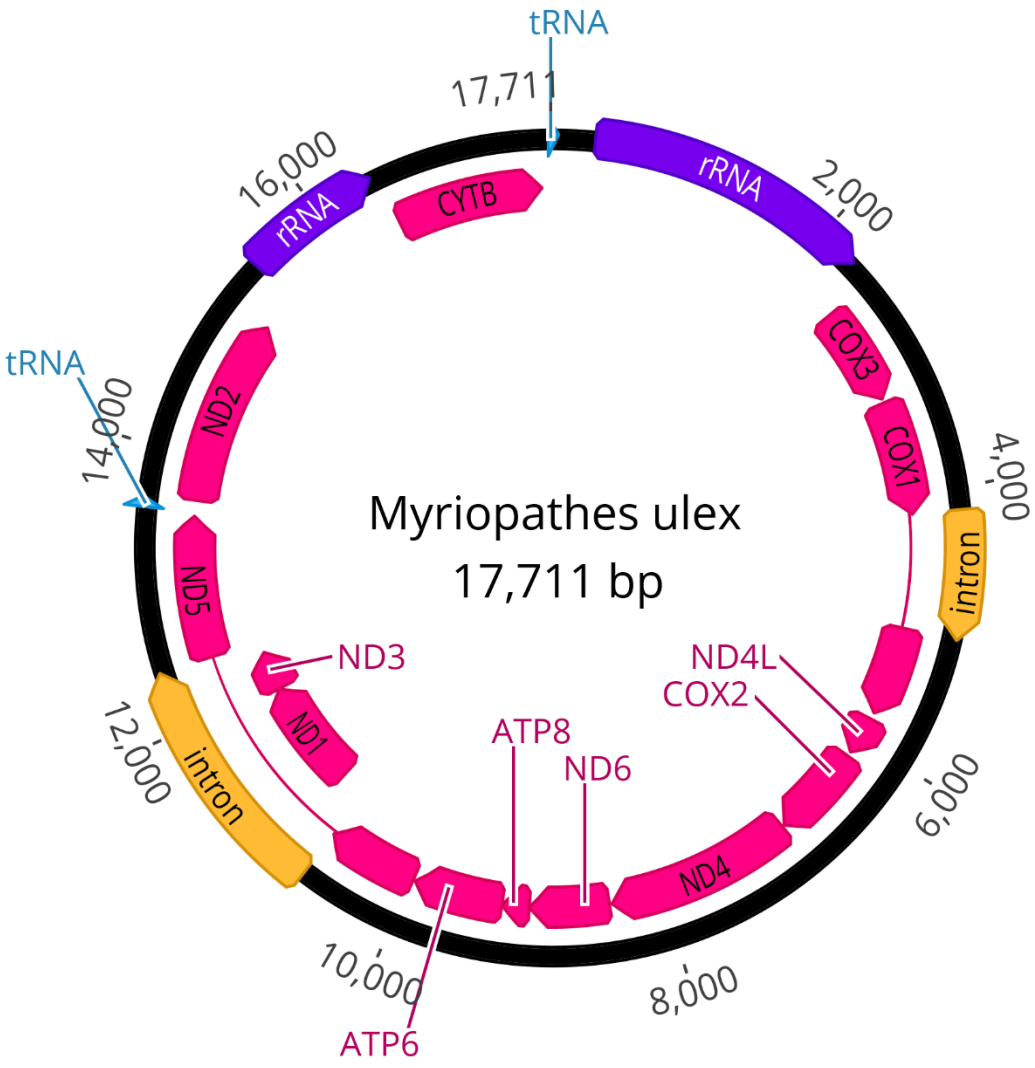

Figure S2.7. Map of the complete mitochondrial genome of *Myriopathes ulex* (#144), drawn by Geneious Prime version 2023.2.1 (https://www.geneious.com).

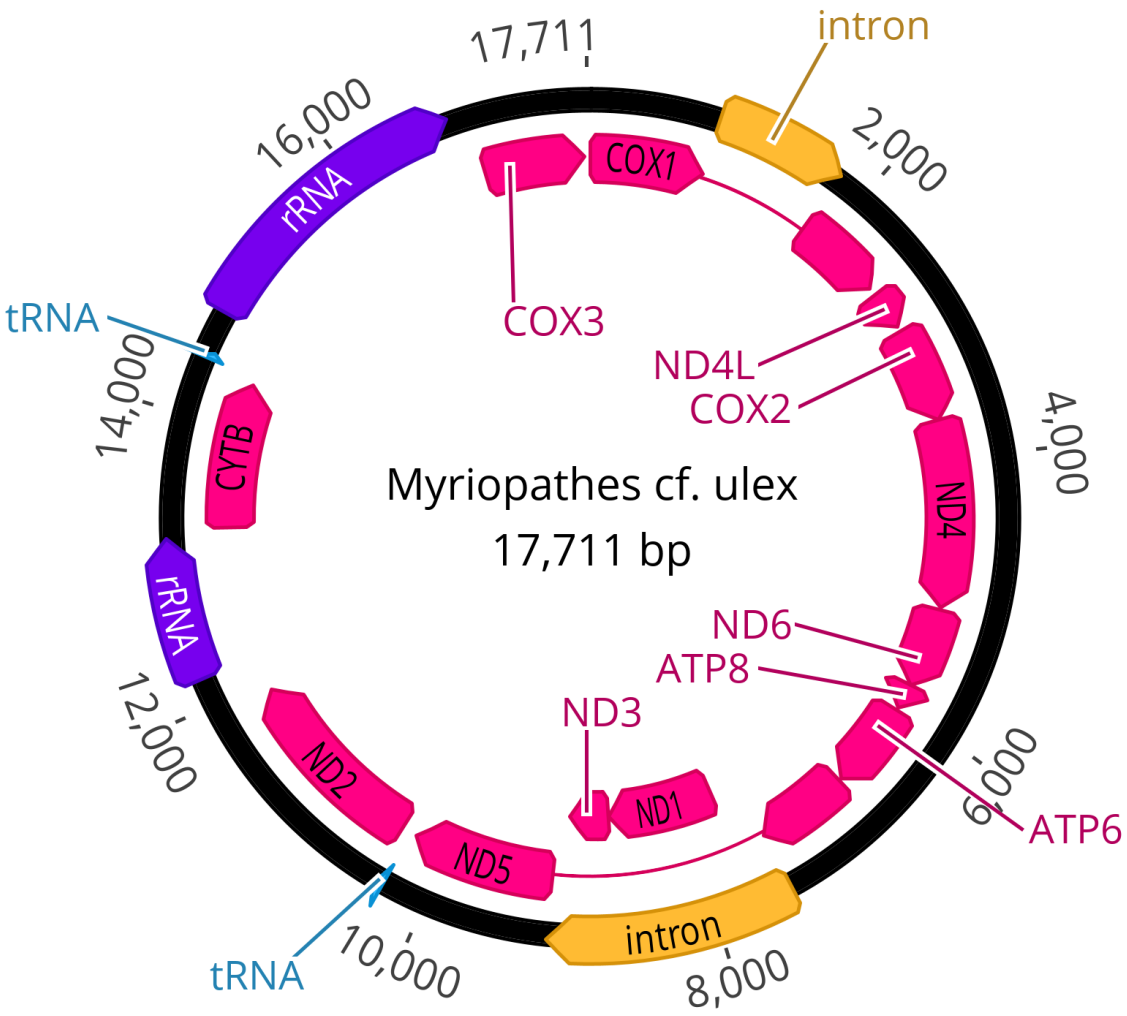

Figure S2.8. Map of the complete mitochondrial genome of *Myriopathes* cf. *ulex* (#269), drawn by Geneious Prime version 2023.2.1 (https://www.geneious.com).

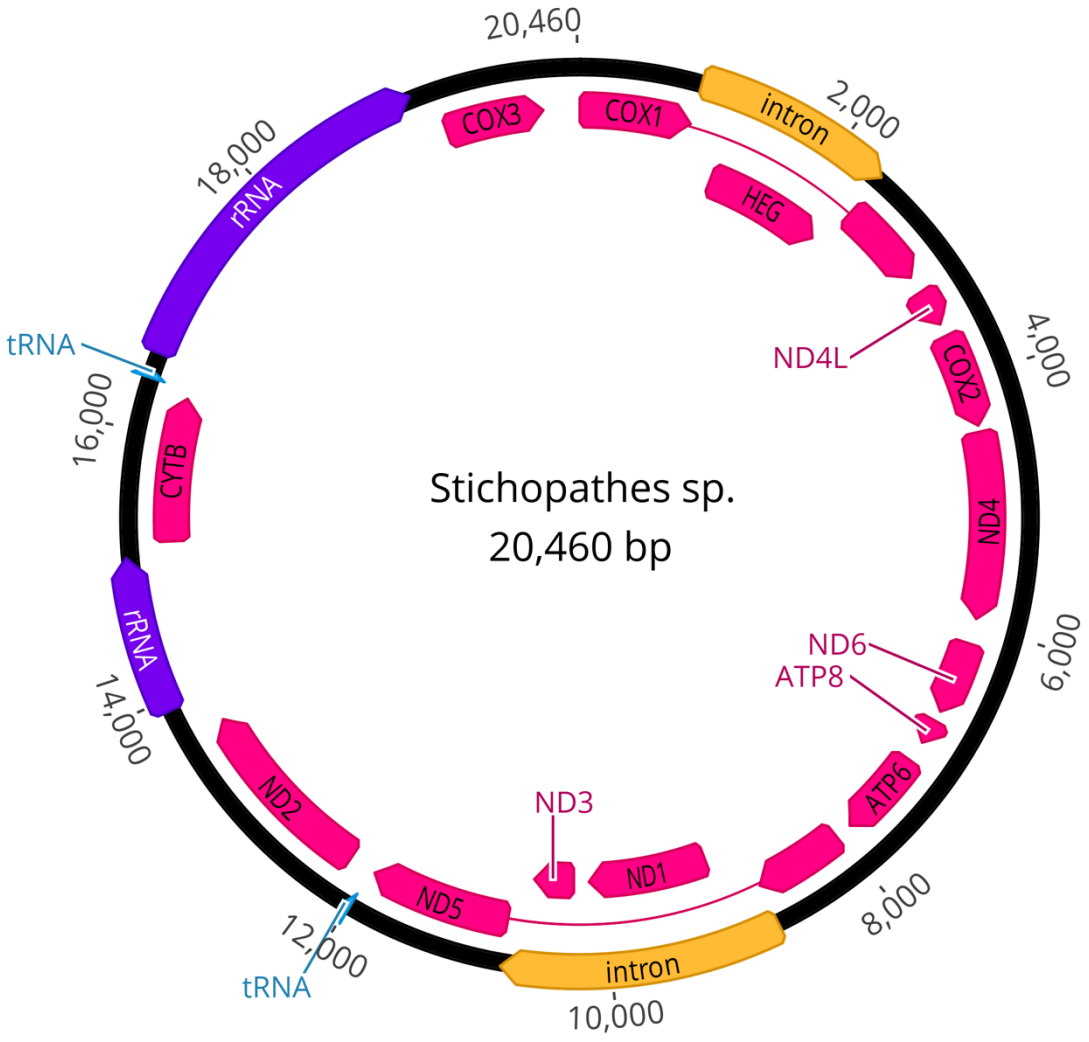

Figure S2.9. Map of the complete mitochondrial genome of *Stichopathes* sp (#180), drawn by Geneious Prime version 2023.2.1 (https://www.geneious.com).

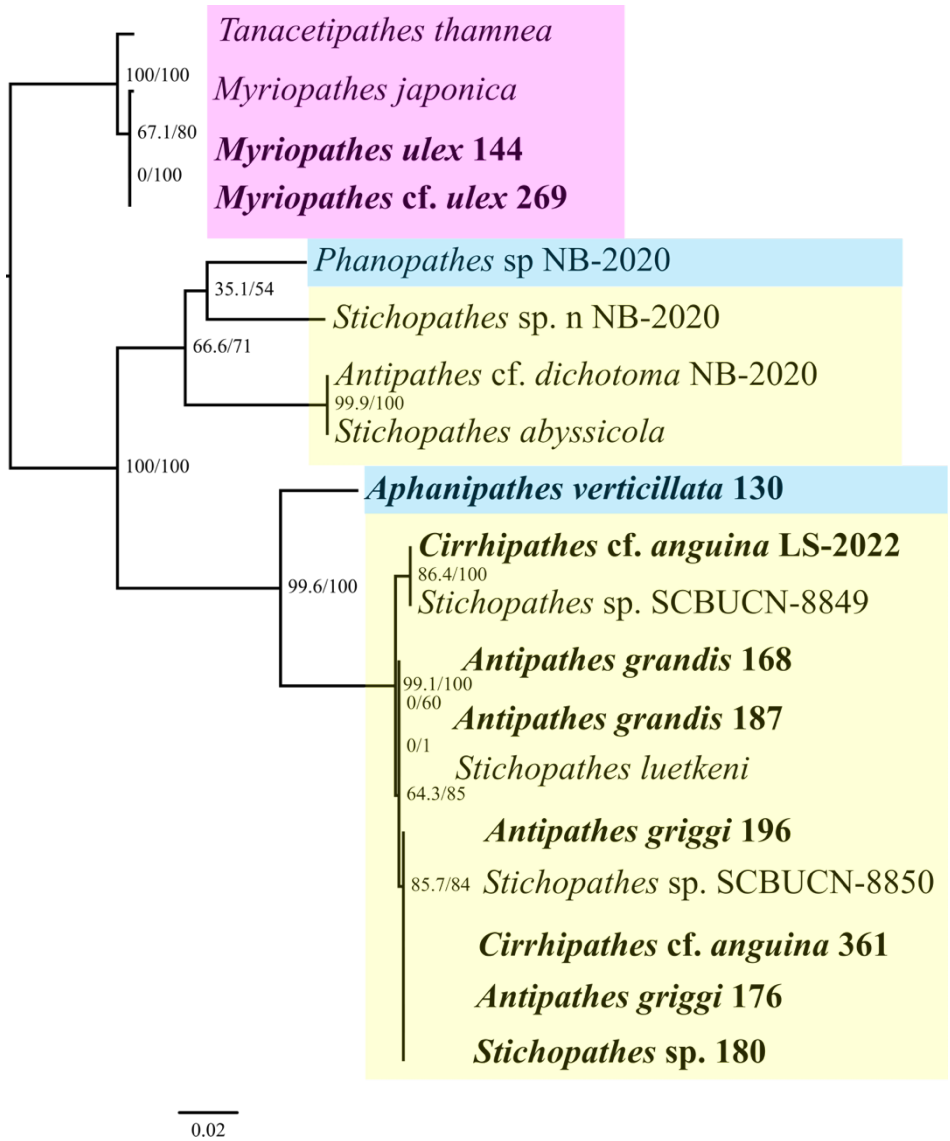

Figure S2.10. Maximum likelihood phylogeny of 19 antipatharian taxa belonging to three families: Myriopathidae (pink), Antipathidae (yellow), and Aphanipathidae (blue). The IQ-TREE inferred phylogeny is based on *ATP6* (pairwise identity: 92.6%; identical sites: 76.4%). ʻĒkaha kū mona sequenced from Hawaiʻi are bolded. Branch lengths are relative to genetic divergence, and values at each node represent SH-aLRT /ultrafast bootstrap values.

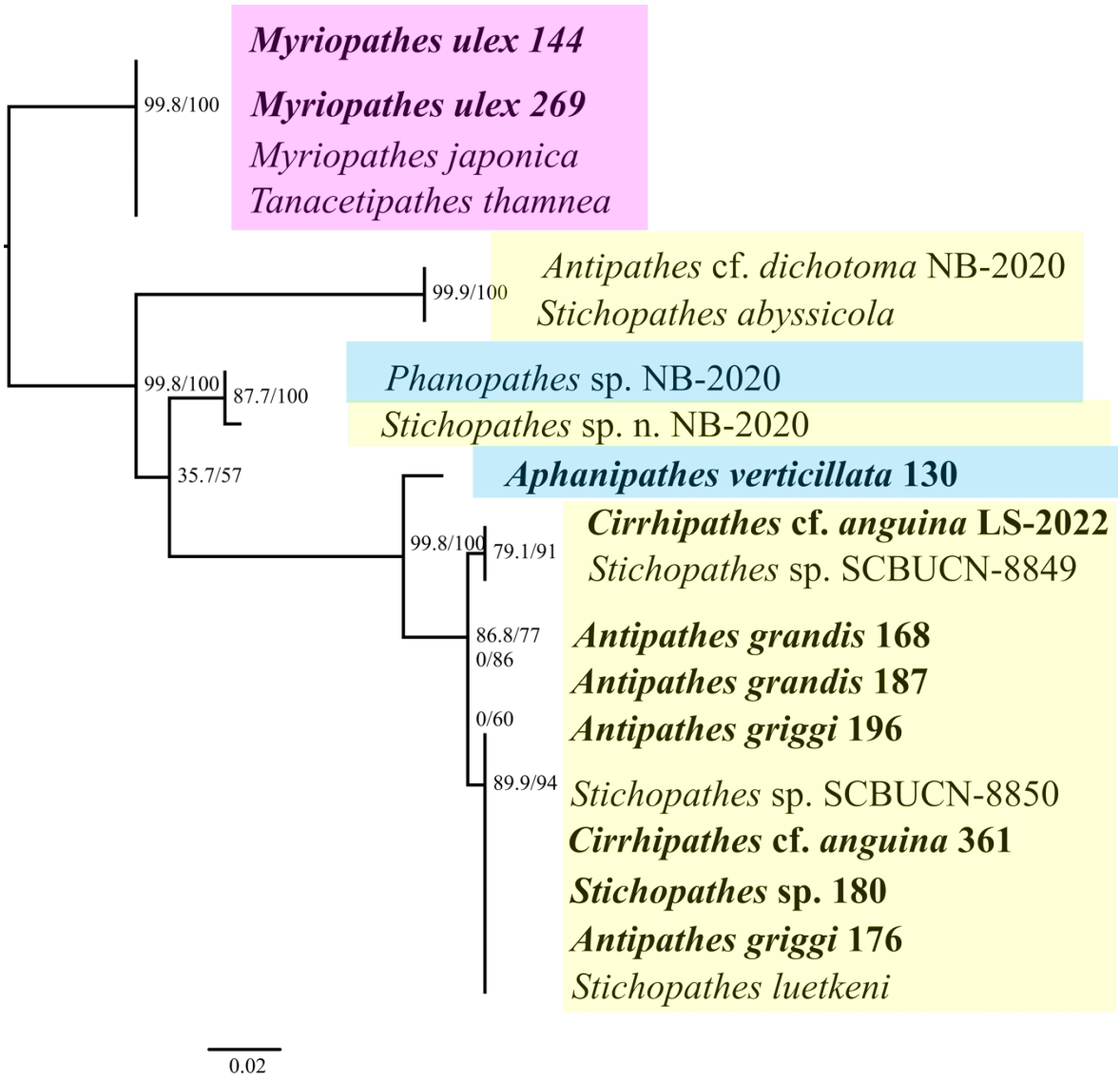

Figure S2.11. Maximum likelihood phylogeny of 19 antipatharian taxa belonging to three families: Myriopathidae (pink), Antipathidae (yellow), and Aphanipathidae (blue). The IQ-TREE inferred phylogeny is based on *ATP8* (pairwise identity: 91.8%; identical sites: 76.5%). ʻĒkaha kū mona sequenced from Hawaiʻi are bolded. Branch lengths are relative to genetic divergence, and values at each node represent SH-aLRT /ultrafast bootstrap values.

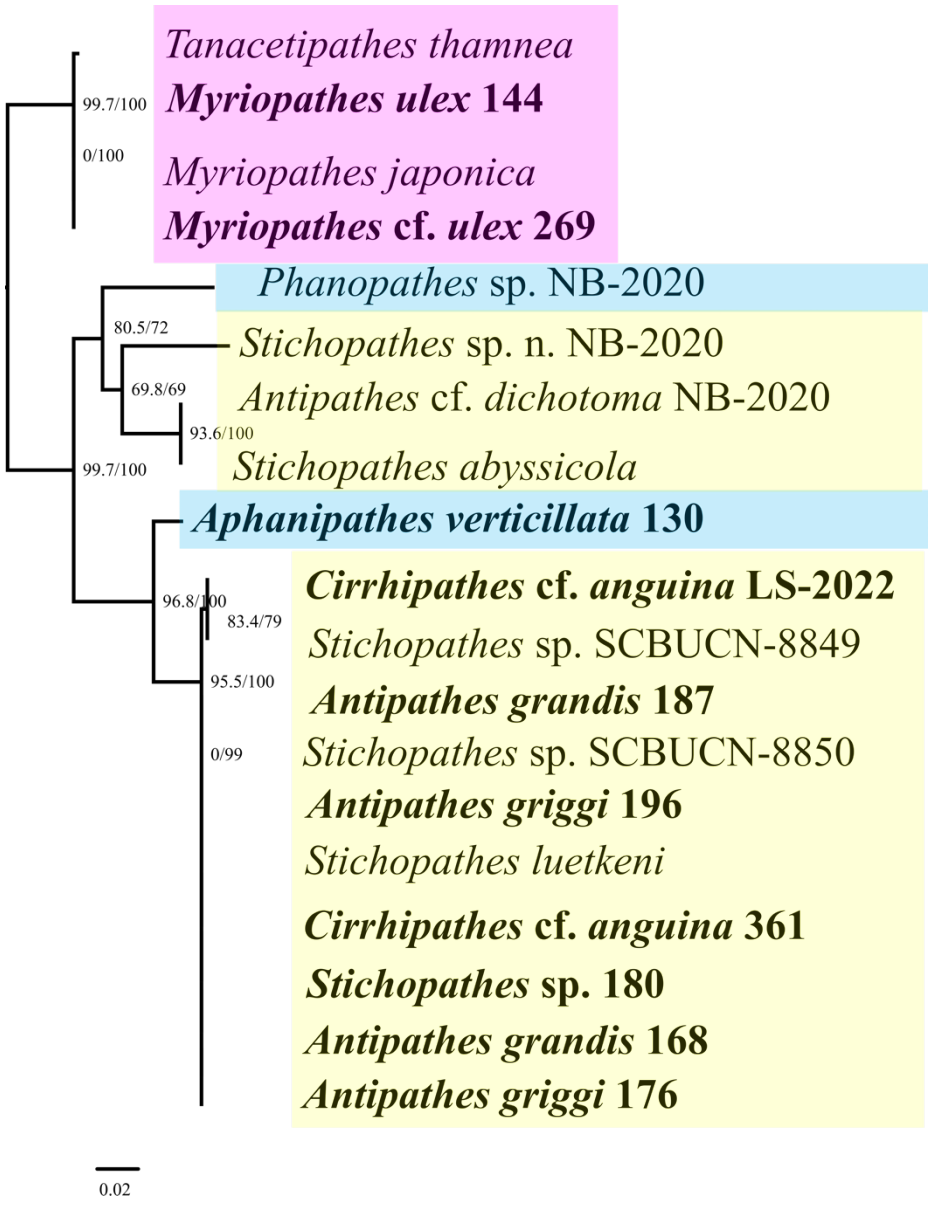

Figure S2.12. Maximum likelihood phylogeny of 19 antipatharian taxa belonging to three families: Myriopathidae (pink), Antipathidae (yellow), and Aphanipathidae (blue). This IQ-TREE inferred phylogeny is based on *ND3* (pairwise identity: 94.1%; identical sites: 81.2%). ʻĒkaha kū mona sequenced from Hawaiʻi are bolded. Branch lengths are relative to genetic divergence, and values at each node represent SH-aLRT /ultrafast bootstrap values.

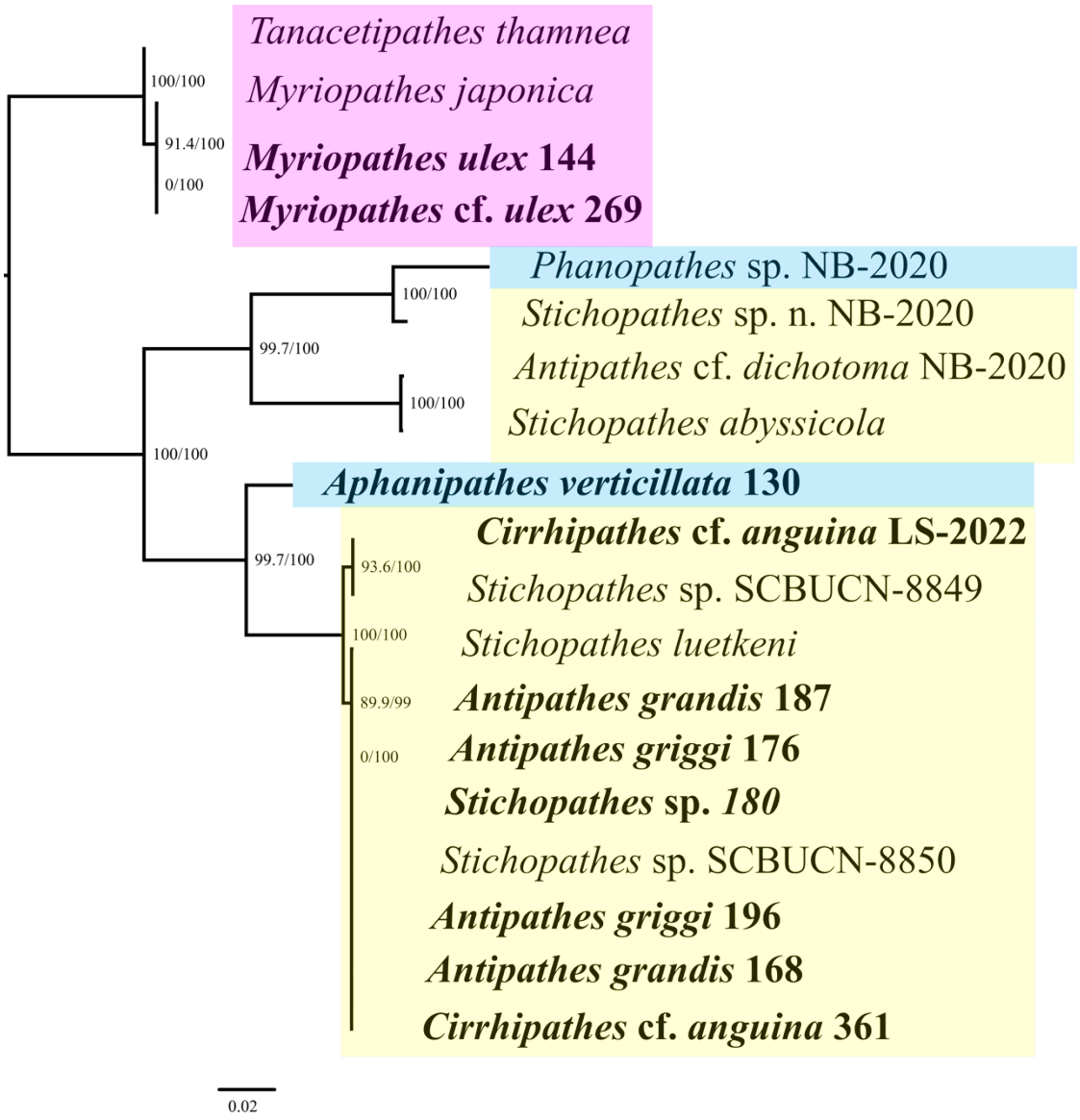

Figure S2.13. Maximum likelihood phylogeny of 19 antipatharian taxa belonging to three families: Myriopathidae (pink), Antipathidae (yellow), and Aphanipathidae (blue). That IQ-TREE inferred phylogeny is based on *ND4* (pairwise identity: 92.1%; identical sites: 76.4%). ʻĒkaha kū mona sequenced from Hawaiʻi are bolded. Branch lengths are relative to genetic divergence, and values at each node represent SH-aLRT /ultrafast bootstrap values.

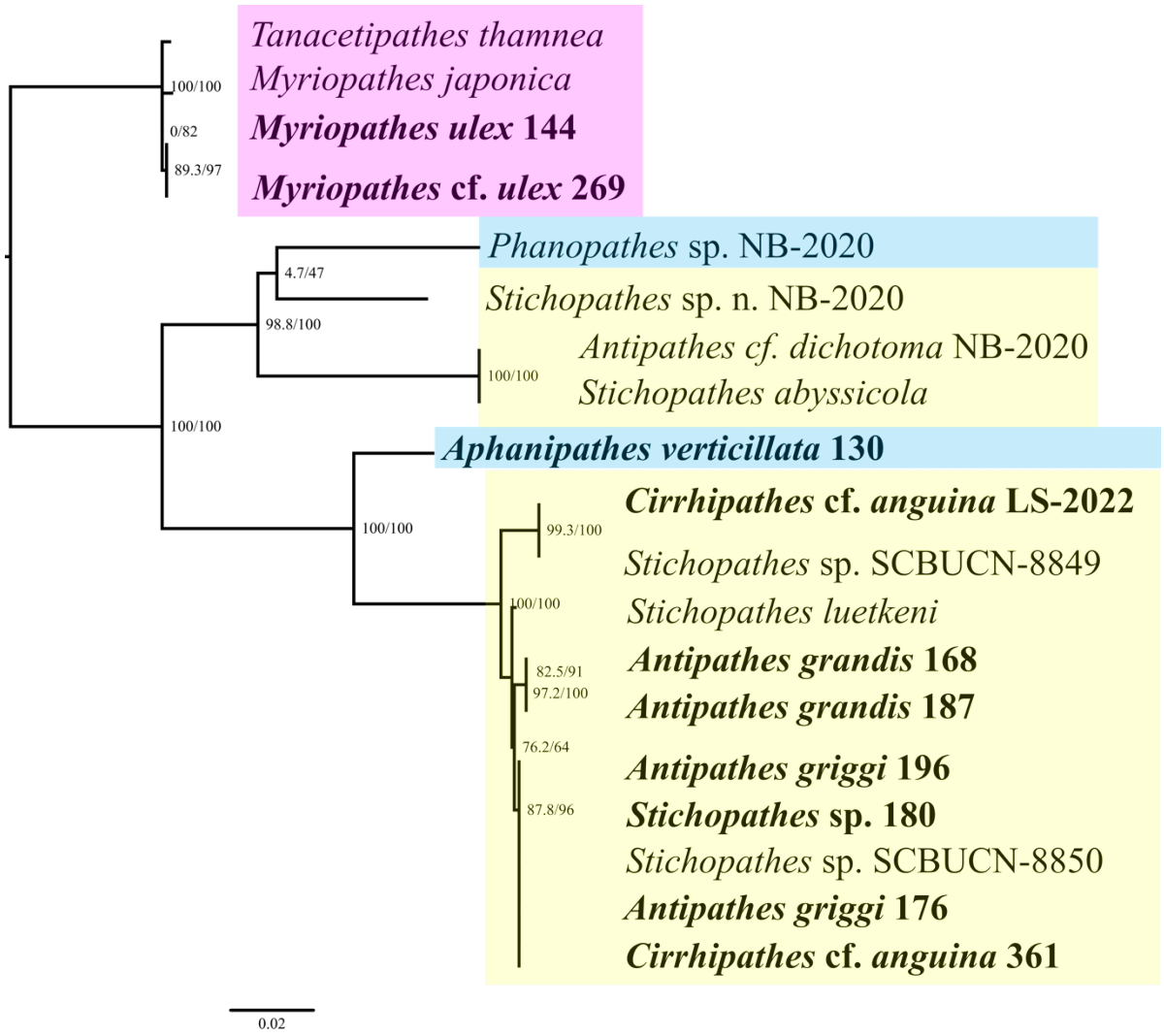

Figure S2.14. Maximum likelihood phylogeny of 19 antipatharian taxa belonging to three families: Myriopathidae (pink), Antipathidae (yellow), and Aphanipathidae (blue). The IQ-TREE inferred phylogeny is based on *ND5* (pairwise identity: 77.1%; identical sites: 36.1%). ʻĒkaha kū mona sequenced from Hawaiʻi are bolded. Branch lengths are relative to genetic divergence, and values at each node represent SH-aLRT /ultrafast bootstrap values.

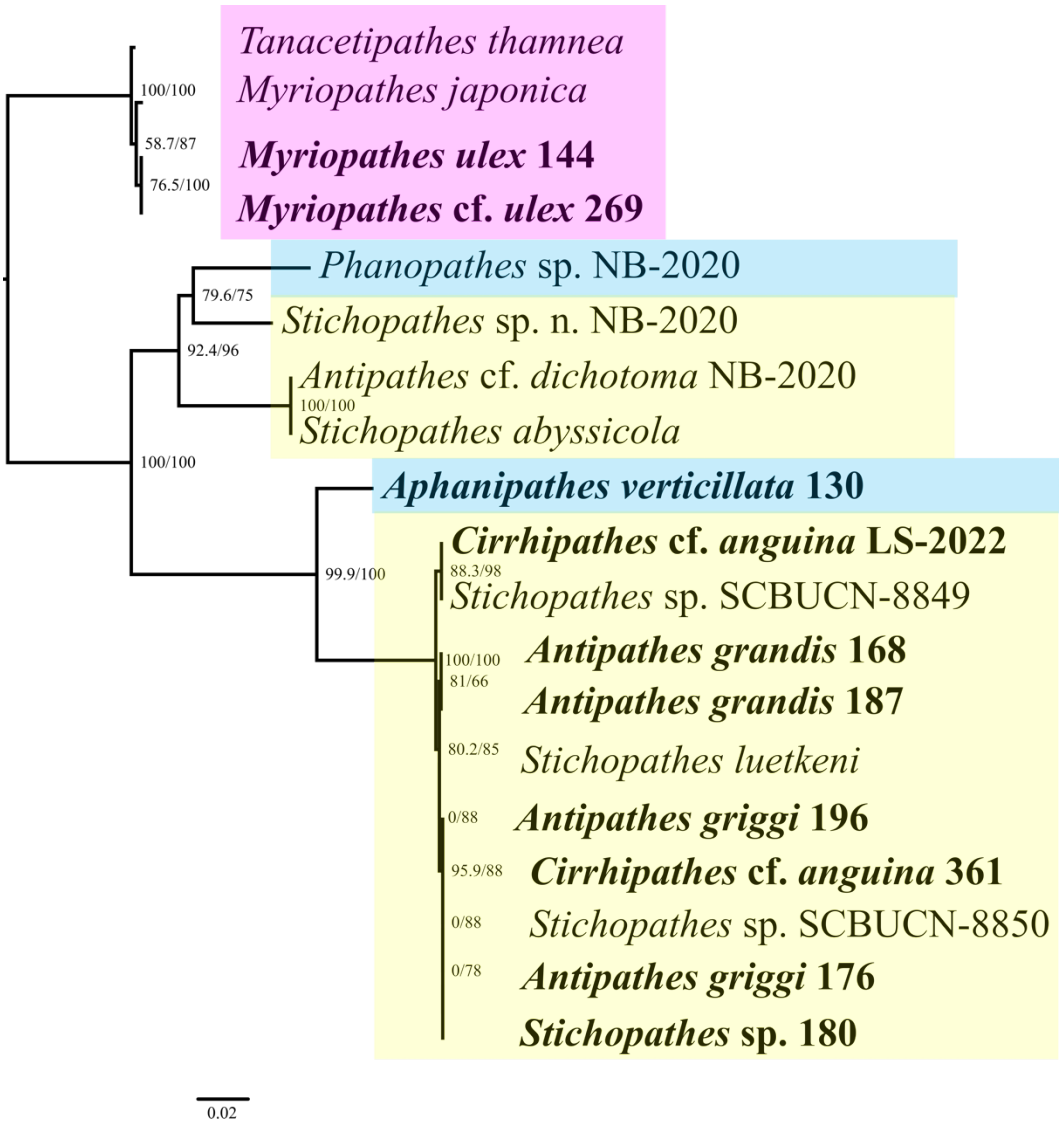

Figure S2.15. Maximum likelihood phylogeny of 19 antipatharian taxa belonging to three families: Myriopathidae (pink), Antipathidae (yellow), and Aphanipathidae (blue). This IQ-TREE inferred phylogeny is based on *COX1* (pairwise identity: 85.3%; identical sites%: 47.4%). ʻĒkaha kū mona sequenced from Hawaiʻi are bolded. Branch lengths are relative to genetic divergence, and values at each node represent SH-aLRT /ultrafast bootstrap values.

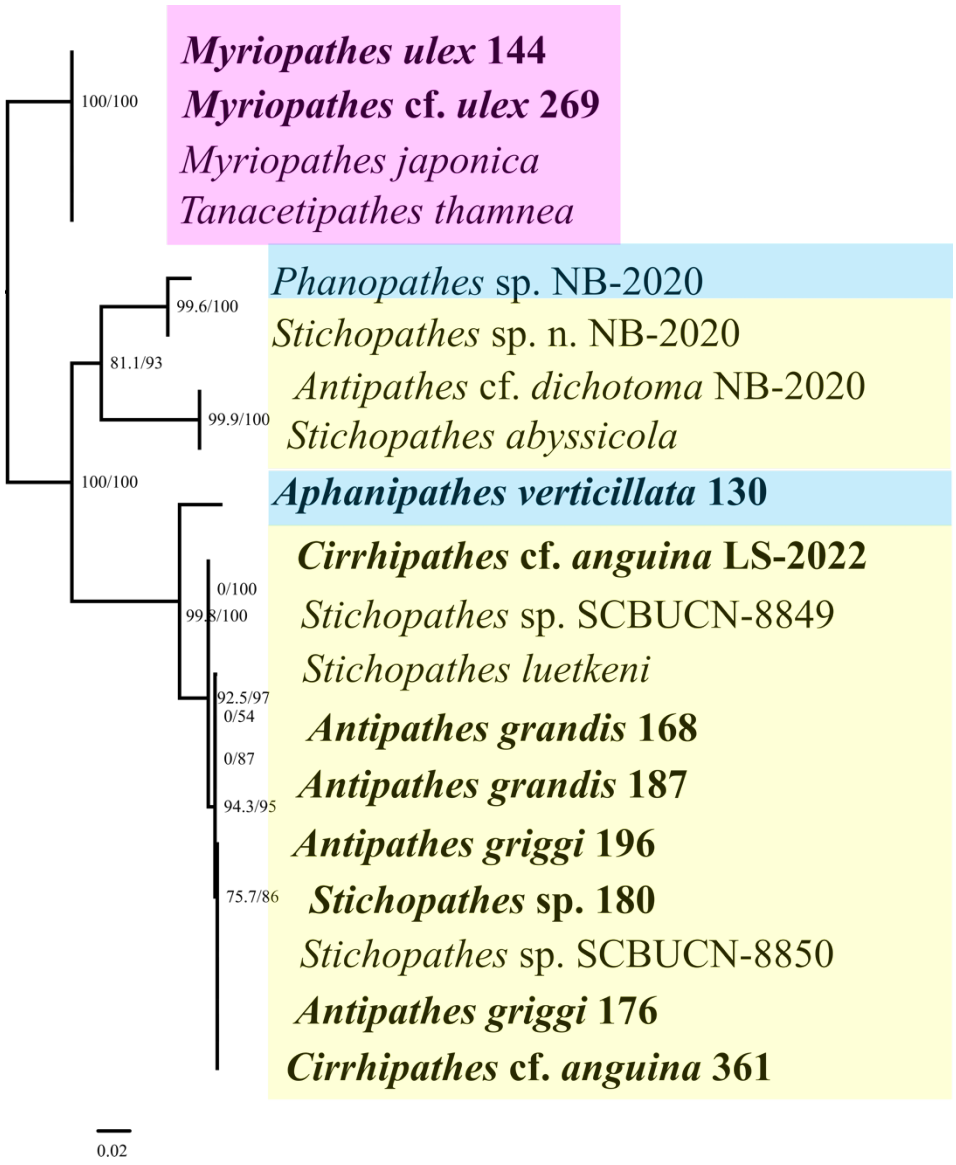

Figure S2.16. Maximum likelihood phylogeny of 19 antipatharian taxa belonging to three families: Myriopathidae (pink), Antipathidae (yellow), and Aphanipathidae (blue). This IQ-TREE inferred phylogeny is based on *COX2* (pairwise identity: 92.6%; identical sites: 78.7%). ʻĒkaha kū mona sequenced from Hawaiʻi are bolded. Branch lengths are relative to genetic divergence, and values at each node represent SH-aLRT /ultrafast bootstrap values.

APPENDIX C: SCRIPT FOR DE NOVO GENOME ASSEMBLY

```
#!/bin/bash
#Script to trim & filter raw reads and produce then evaluate a de novo genome assembly
#Written by Evan W. Barba, modified by Leah E.K. Shizuru
#This pipeline depends on:
#Trim Galore! http://www.bioinformatics.babraham.ac.uk/projects/trim_galore/
#SPAdes https://github.com/ablab/spades
#QUAST https://github.com/ablab/quast

###Begin Code###

        if [ ! -d "trim_galore" ]; then
                mkdir trim_galore
                        fi

#cd into the directory where fastq.gz files are located and employ the following to batch process on pair-end fastq.gz files
#files had the following naming scheme: "sampleID_raw_F.fastq.gz" and "sampleID_raw_R.fastq.gz"
#brace expansion enables Trim Galore! to grab all files that are named _raw_F.fastq.gz and _raw_R.fastq.gz and apply the specified trimming parameters

        find -name "*_raw_F.fastq.gz" | cut -d "_" -f1 | parallel trim_galore --illumina --paired --retain_unpaired --fastqc -o trim_galore/ {}\_raw_F.fastq.gz {}\_raw_R.fastq.gz

        find ./ -name "*.F.fq.gz" | cut -d "." -f2 | sed 's/\///' > popslist

#SPAdes:
```

```
        spades.py --careful -t 30 -m 300 -o /data/leah/spades/`sampleID` -1
        `forward_trimmed_read` -2 `reverse_trimmed_read`

# QUAST:

        if [ ! -d "quast" ]; then
                mkdir quast
                        fi

        KMER=(` find ./ -maxdepth 1 -name "K*" | cat  `)
                ls K* -d | parallel -j 30 cp ./{}/final_contigs.fasta ./quast/{}.fasta

        cd quast

        quast.py -e -t 30 -m 300 ../contigs.fasta "${KMER[@]/%/.fasta}"

#create "large_contigs.fasta"

        sed ':a;N;/^>/M!s/\n//;ta;P;D'  contigs.fasta > sed_corr.fasta

        awk '/^>/ { getline seq } length(seq) >10000 { print $0 "\n" seq }' sed_corr.fasta >
        large_contigs.fasta

#BLAST large_contigs.fasta as a secondary check for assembly
```

APPENDIX D: IQ-TREE PARTITION COMMANDS

RaxML-style partition commands used for IQ-TREE analysis in Chapter 1

```
#NEXUS
begin sets;
        charset ATP6 = 1-717;
        charset ATP8 = 718-939;
        charset COX1 = 940-4295;
        charset COX2 = 4296-5048;
        charset COX3 = 5049-5837;
        charset CYTB = 5838-7025;
        charset ND1  = 7026-8102;
        charset ND2  = 8103-9677;
        charset ND3  = 9678-10037;
        charset ND4  = 10038-11540;
        charset ND4L = 11541-11840;
        charset ND5  = 11841-16153;
        charset ND6  = 16154-16822;
end;
```

RaxML-style partition commands used for IQ-TREE analysis in Chapter 2

```
#NEXUS
begin sets;
        charset ATP6 = 1-702;
        charset ATP8 = 703-915;
        charset COX1 = 916-3436;
        charset COX2 = 3437-4186;
        charset COX3 = 4187-4975;
        charset CYTB = 4976-6118;
        charset ND1  = 6119-7169;
        charset ND2  = 7170-8744;
        charset ND3  = 8745-9128;
        charset ND4  = 9129-10604;
        charset ND4L = 10605-10904;
        charset ND5  = 10905-14928;
        charset ND6  = 14929-15573;
end;
```

APPENDIX E: SCRIPT FOR IQ-TREE

```
#!/bin/bash
#Script used for IQ-Tree

Iqtree -s /`path to alignment in .fasta format` -p /`path to partitions.nex` -m MFP+MERGE -B
1000 -alrt 1000 -bnni -T auto
```